Simulation and optimization of novel configurations of triple absorption heat transformer integrated to a water desalination system

Mehrdad Khamooshi

Submitted to the
Institute of Graduate Studies and Research
in partial fulfillment of the requirements for the Degree of

Master of Science
in
Mechanical Engineering

Eastern Mediterranean University
January 2014
Gazimağusa, North Cyprus

Approval of the Institute of Graduate Studies and Research

Prof. Dr. ElvanYılmaz
Director

I certify that this thesis satisfies the requirements as a thesis for the degree of Master of Science in Mechanical Engineering.

Prof. Dr. Uğur Atikol
Chair, Department of Mechanical Engineering

We certify that we have read this thesis and that in our opinion it is fully adequate in scope and quality as a thesis for the degree of Master of Science in Mechanical Engineering.

Prof. Dr. Mortaza Yari
Co-Supervisor

Prof. Dr. Fuat Egelioğlu
Supervisor

Examining Committee

1. Prof. Dr. Fuat Egelioğlu
2. Prof. Dr. Mortaza Yari
3. Prof. Dr. Uğur Atikol
4. Assoc. Prof. Dr. Hasan Hacışevki
5. Asst. Prof. Dr. Neriman Özada

ABSTRACT

In this study, a thermodynamic analysis on six different configurations of triple absorption heat transformer (TAHT) utilizing lithium bromide and water as the working fluid of the cycle integrated with water desalination system has been conducted. The energy source of the desalination system is provided by high temperature heat of the TAHT which was utilizing the waste heat from a textile factory. A thermodynamic model in Engineering Equation Solver (EES) was developed for the performance analysis of the system such as; coefficient of performance (COP), exergy coefficient of performance (ECOP), quantity of distilled water and utilized heat for the use of desalination. Also an optimization was made with respect to the main parameters of the cycle in order to maximize the amount of the freshwater production rate for all configurations. Six alternative configurations were made by different arrangement of heat exchanger units within the system. It is found that last modified configuration can increase the COP and production rate of fresh water compared with other configurations. The results show that the optimized amount of water output obtained from the last proposed configuration was 0.1307 kg/s which is enough to supply 1131 residential units.

Keywords*:* Triple absorption heat transformer, $LiBr/H_2O$, Desalination, economizer

ÖZ

Bu çalışmada, lityum bromür ve suyu çalışma akışkanı olarak kullanan su arıtma sistemi ile entegre üçlü emilim ısı trafo (ÜEIT) çevriminin on altı farklı konfigürasyonda termodinamik analizi yapıldı. Su arıtma sisteminin enerji kaynağı bir tekstil fabrikasındaki atık ısıyı kullanan ÜEIT den gelen yüksek sıcaklıktaki ısıdan sağlanmaktadır. Engineering Equation Solver (EES) yazılımı kullanılarak sistemin performans analizleri için termodinamik model geliştirildi örneğin; etkinlik katsayısı, ekserji etkinlik katsayısı, damıtılmış su miktarı ve damıtmada kullanılan ısının analizi. Ayrıca, tatlı su üretimini maksimize etmek için çevrimin temel parametreleri kullanılarak tüm konfigürasyonların optimizasyonu yapıldı. Sistem içerisinde ısı eşanjörlerinin farklı düzenlenmesi ile altı alternatif konfigürasyon yapıldı. Son konfigürasyondaki (6. Konfigürasyon) etkinlik katsayısı ve tatlı su üretimi diğer düzenlemelere göre daha yüksek bulunmuştur. Sonuçlar son önerilen konfigürasyonda elde edilen optimize edilmiş su üretim miktarının 0.1307 kg/s, bunun 1131 konut için yeterli olduğunu göstermektedir

Anahtar Kelimeler: üçlü emilim ısı trafo, LiBr/H_2O, Su arıtma, ısı eşanjörü

***This thesis is dedicated to my family for their love, endless support and encouragements*.**

ACKNOWLEDGMENT

I would like to declare my sincere gratitude to my supervisor Prof. Dr. Fuat Egelioglu for continuous support of my M.Sc. thesis, for his patience and his immense knowledge. I would like to thank him for encouraging my research and for allowing me to become a researcher. Beside my supervisor, I am grateful to my co-supervisor Assoc. Prof. Dr. Morteza Yari for his encouragement, insightful comments and motivation.

My sincere and thanks belong to my dear friend Kiyan Parham for offering and providing opportunities and topics for my research activities. His support and advice throughout the research are greatly appreciated. In fact, without his guidance, I would not be able to reach to this situation.

TABLE OF CONTENTS

LIST OF TABLES

LIST OF FIGURES

LIST OF ABRIVATIONS

abs	Absorber
AB/EV	Absorber/evaporator
con	Condenser
COP	Coefficient of Performance
DAHT	Double Absorption Heat Transformer
ECOP	Exergetic Coefficient of Performance
eva	Evaporator
gen	Generator
GTL	Gross Temperature Lift
HEX	Heat Exchanger
SAHT	Single absorption heat transformer
TAHT	Triple absorption heat transformer

LIST OF SYMBOLS

ε	Economizer effectiveness(dimensionless)
X	Concentration
f	Flow ratio
T	Temperature (^{o}C)
P	Pressure (kPa)
Q	Heat Capacity (kw)
ṁ	Mass flow rate (kg/s)
h	Entalphy (kJ/kg)

LIST OF SUBSCRIPTS

O	Ambient
S	Strong
w	Weak
u	Utilized

Chapter 1

INTRODUCTION

1.1 Clean water

Earth seems to be unique among other planets due to the fact that water is essential for its survival. The dependency of life on fresh water is so crucial that without it the world would confront devastating crises. A great majority of the earth's surface is covered with water but only 2.5% of this huge amount of water is fresh water and most of the remaining parts are salty water found in the oceans [1, 2]. Desalination techniques that can be used for water purification are capable of providing fresh water from the salty waters in the oceans. The distillation procedures can separate water and dissolved substance by evaporating and then again condensing it [3]. An external thermal energy source which can be supplied by many sources such as solar energy [4], geothermal [5], nuclear energy [6], absorption heat transformer [7, 8] is needed for evaporating the water. Detecting and providing the suitable thermal energy source for the desalination systems has become a subject for researchers throughout decades.

1.2 Utilization of the waste heat

Huge amount of low or mid-level waste heat are released daily from industrial processes to the atmosphere [9]. There are thermodynamic cycles which can recover these low grade waste heats such as Organic Rankine cycle (ORC) and CO_2

Transcritical power cycle (CDTPC). ORC and CDTPC can efficiently convert low-temperature waste heat into electricity [10, 11].

In the desalination systems the temperature of the mid-level waste heats should be increased for higher yields. For a better effectiveness AHTs which are capable of upgrading the energy effectiveness of industrial applications appear to be a noble choice for utilizing these waste heats. AHTs are systems which can convey heat at higher temperatures rather than that of original temperature of the source. They are systems having opposite operation process of Absorption Heat Pumps (AHPs). Due to the fact that the basic operation of the AHTs are close to AHPs, AHTs will have the same advantages of the absorption systems such as: quite operation, low maintenance requirement, low mechanical work input and simple design [12]. The upgraded heat for example can satisfy the need of thermal energy sources for the distillation processes. Numerous researchers have been investigating different configuration of absorption heat transformers integrated to water purification processes throughout the recent decades.

1.3 Motivation

Due to the lack and continuously increasing demand for fresh water in the world and loss of waste heats from industrial processes to atmosphere, makes it essential to investigate the feasibility of AHTs integrated to water desalination system. By utilizing waste heat for water desalination the fresh water scarcity will decrease. A broad range of studies has been performed about analyzing the SAHT and DAHT coupled to water desalination system. This study attempted to simulate the performance of a TAHT integrated with water desalination system, very few studies

were performed for TAHT and in those studies upgraded heat of THAT was not used for the aim of desalination.

1.4 Thesis Objectives

In this study the primary objective is to evaluate the performance of various TAHT configurations in which the enhanced temperature is used for the aim of water desalination. A complete thermodynamic analyses and effectiveness evaluation of the six different configurations will be performed. The main objective is to investigate the effect of some parameters such as; temperature of the main components (absorber, condenser, generator, evaporator, first absorber/evaporator (AB/EV1) and second absorber/evaporator (AB/EV2), weak and strong solutions' concentration, heat exchanger effectiveness on the performance of the cycle and the production of fresh water. A parametric study is performed and the developed model was also validated with the theoretical and experimental data from [13, 14]. Furthermore the all the configurations are thermodynamically optimized using the EES software [15].

Chapter 2

DIFFERENT TYPES OF ABSORPTION HEAT TRANSFORMERS

2.1 Definition of Absorption Heat Transformer

Single absorption heat transformers are usually consisted of a generator, condenser, evaporator, absorber and a heat exchanger. Heat is transferred to the working fluid (LiBr/H2O) from the generator and evaporator by utilizing the waste heat from industry. Figure 2.1 shows a single absorption heat transformer (SAHT) diagram.

In a SAHT heat from a heat source supplied to separate the working fluid in the generator. Superheated water vapor which is the refrigerant exits the generator at state 1 (see Fig 2.1) and enters to the condenser where it is condensed to saturated liquid. The pressure of condensed refrigerant is increased to evaporator pressure by a refrigeration pump (state 3). In the evaporator water is heated to saturated vapor phase with the same heat provided to the generator. This vapor is absorbed in the absorber by strong LiBr/H_2O solution from the generator and an exothermic reaction in the absorber increases the temperature of the solution approximately by 30-60 °C compared with the generator temperature. The released heat from the reaction is transferred to brackish water as latent and sensible heat in the desalination system. The weak solution exiting the absorber to the generator is utilized for preheating the strong solution from generator to absorber via the heat exchanger (HEX).

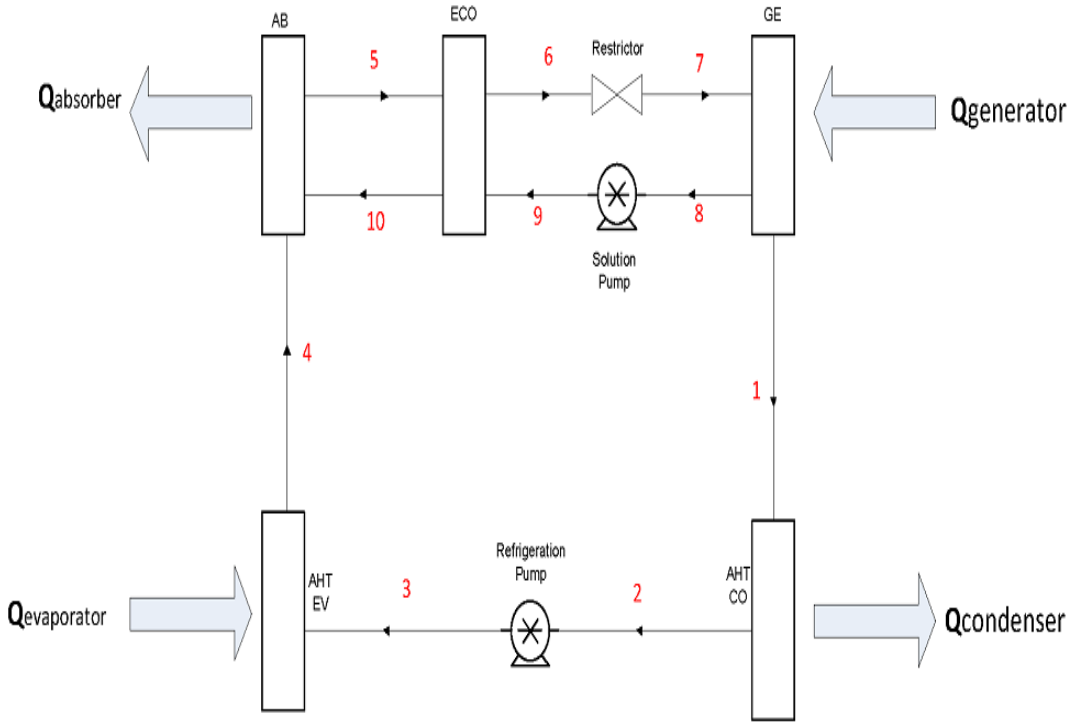

Figure 2.1. Schematic diagram of single absorption heat transformer

The amount of gross temperature lift ($GTL=T_{abs}-T_{gen}$) basically depends on the additional stages added to the SAHTs. Table 1 shows the (COP) and GTL of different types of absorption heat transformers.

Table 2.1 From the various studies system performances of different type of absorption heat transformers

Type	GTL	COP	Ref. No
Single absorption heat transformer (SAHT)	50 °C	~0.5	[9, 16, 17]
Double absorption heat transformer (DAHT)	80 °C	~0.35	[16, 18, 19]
Triple absorption heat transformer (TAHT)	~140	~0.23	[13, 20]

2.2 Single Absorption Heat Transformer

Different configurations of SAHTs with $LiBr/H_2O$ as the working fluid were investigated by Horuz and Kurt [9]. It was concluded that modified configuration presented by Horuz and Kurt [9] could increase the COP by 14.1% compared to the basic AHT. In addition to this study Parham et al. [17] presented a study with the aim of simulating and optimization of the similar configurations used in [9] integrated to a water desalination process. The final configuration was capable of producing pure water at a rate of 0.2435 kg/s. A cogeneration system consisted of a 5 kW proton exchange membrane fuel cell (PEMFC) and a SAHT was investigated by Huicochea et al. [21]. Huicochea et al. obtained results showing that the COP could reach to 0.256 and the combined system of SAHT and PEMFC was a feasible project.

Sekar and Seravanan [22] carried out an experimental study on the combination of a SAHT with lithium bromide and water coupled to a 5 kg/h distilled water capacity distillation unit. The result indicates that the COP of the system was dependent on the heat source temperature. GTL and the maximum COP were indicated as 20 °C, 0.38, respectively. A thermodynamic and corrosion system with an on-line data acquisition model was used by Escobar et al. [23] in order to optimize the long term performance of an AHT integrated to a water purification process. By applying this system stopping the process when an extreme corrosion attack was occurred in the main components was made possible. A comparison was made by Hernandez et al. [24] between performance prediction of the SAHT coupled with a desalination system by a neural network model (NnM) and a thermodynamic model (ThM). They concluded that the NnM for COP estimation model was very accurate as experimental results are in good agreement with NnM results.

Siqueiros and Romero [25, 26] conducted two studies about recycling energy assuming constant and increasing heat source temperature. They noticed some improvements in the proposed cycles than that of a simple AHT.

Sozen and Yucesu [27] developed a mathematical model for comparing the system performance of the AHT with ejector to the SAHT without ejector. Both cycles used H_2O/NH_3 as the working fluid and utilized the waste heat from a solar pond. The outcomes demonstrated that both energy and exergy effectiveness improvement were achievable by using an ejector in the absorption heat transformer.

A new combined cogeneration system consisting of a single absorption heat transformer and two ORCs were proposed by Zare et al. [28]. The required power for

this system was provided by the waste heat of a gas turbine-modular helium reactor (GT-MHR). They demonstrated that the COP and the water production rate have direct relations with the heat source temperature of the AHT. Yari presented a novel cogeneration cycle comprised of CDTPC and a SAHT with lithium bromide and water solution [29]. Yari indicated that the maximum water production rate of 3.317kg/s was acquired by the cycle.

The performance of the absorption cycles not only depend on their configuration, but also on the thermodynamic properties of working pairs which are regularly composed of refrigerants and absorbents. Sun et al. [30] conducted a review study about different kinds of working pairs in absorption cycles. Furthermore, Khamooshi et al. [31] did a similar work by employing ionic liquids as working fluids. Bourouis et al. [32] simulated a seawater desalination system integrated to a SAHT utilizing H_2O/(LiBr+Lil+LiNO3+LiCl) as the working fluid of the system. The results demonstrated that the system mentioned with working fluid showed a better performance compared with H_2O/LiBr systems.

Zhang and Hu [33] introduced a new working fluid for the absorption heat transformer composed of ionic liquid and water. The new working pair was 1-ethyl-3-methylimidazolium dimethylphosphate, and water (H2O + [EMIM][DMP]). They stated that due to the system's performance and excellent working fluid properties which have advantages such as no crystallization, no corrosion and negligible vapor pressure it had possibility of becoming a successful working fluid. Horuz [34] compared the working fluids H_2O/NH_3 and $LiBr/H_2O$ solutions in SAHT.

2.3 Double Absorption Heat Transformer

Gomri [8] presented the single and double effect AHT systems for seawater desalination. The results indicated higher COP and ECOP for double effect AHT than the single effect AHT. On the contrary, pure water yield of single effect is more than that of double effect AHT coupled to seawater purification process.

Efficiencies of a double absorption heat transformer operating with LiBr/H2O were studied by Martinez and Rivera [35]. They developed a mathematical model for estimating the COP, ECOP, total exergy destruction in the system and in each component as a function of temperature. Horuz and Kurt [16] investigated and compared single, series and parallel double absorption heat transformers. They concluded that the parallel DAHT system could produce more water vapor than that of the series DAHT system.

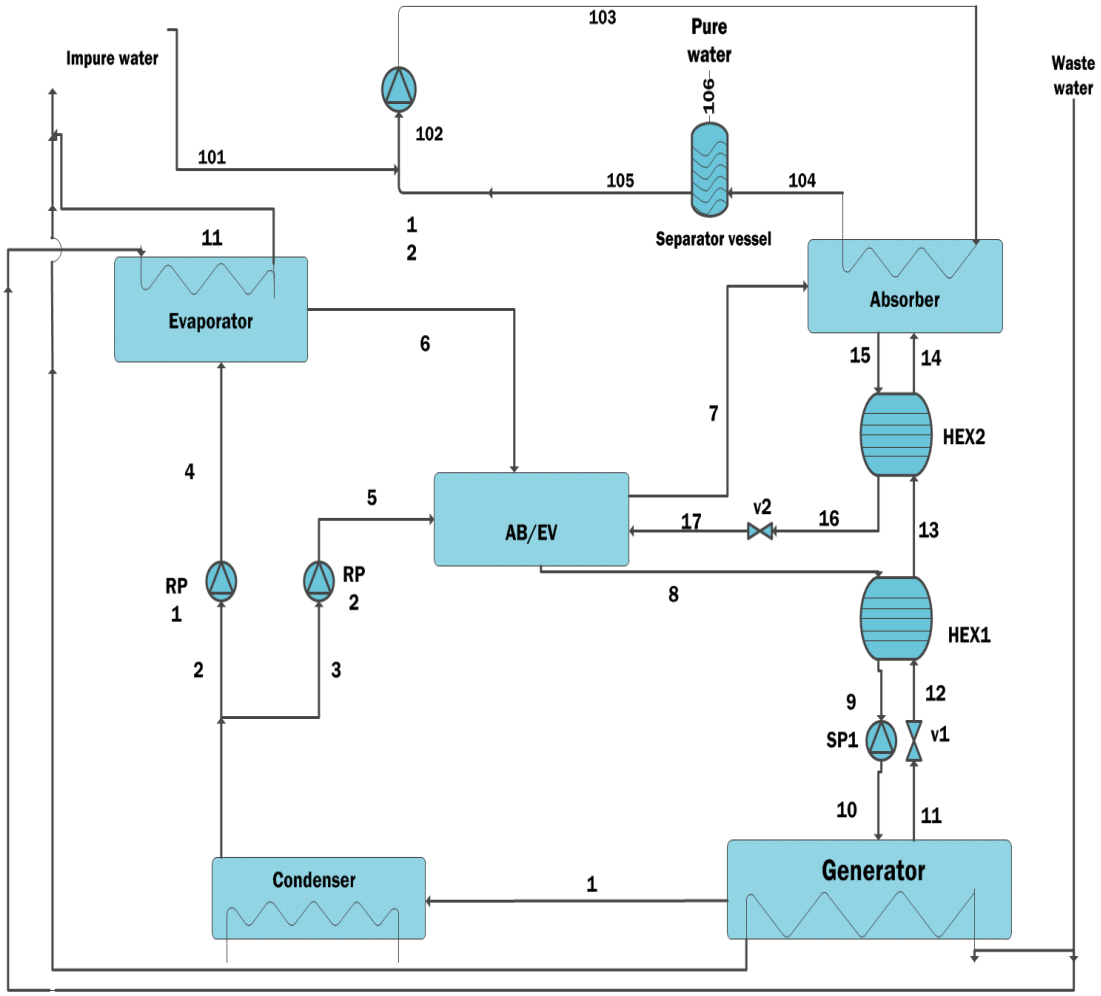

Figure 2.2. Schematic view of double absorption heat transformer integrated to water desalination system

Reyes et al. [36] simulated the performance of SAHT and DAHT by using $H_2O/CaCl_2$ and $H_2O/LiCl$ as the working fluids of the system. $H_2O/LiCl$ showed a better system performance than that of $H_2O/CaCl_2$ pair.

2.4 Triple Absorption Heat Transformer

A rigorous multi-dimensional analysis was made by Donnellan et al. [20] for a conventional triple absorption heat transformer. It was concluded that the condenser temperature should be as low as possible. Donnellan et al.[13] introduced six different configurations of TAHTs applying H2O/LiBr as the working pair. They analyzed and optimized the number and placement of internal HEX units throughout the cycle using heat exchanger network modeling. In the first case the TAHT does

not include any heat exchanger and so the model does not take the benefit of any heat recovery in the cycle. The second case has two additional heat exchangers in the second and third stages of the TAHT. The third case is called the conventional TAHT. It possesses three heat exchangers in any stage of the cycle (where preheating of the strong solution from the generator to both AB/EV and the absorber were done). In the 4^{th} case, changes have been made to the conventional model by applying two splits and one combo.

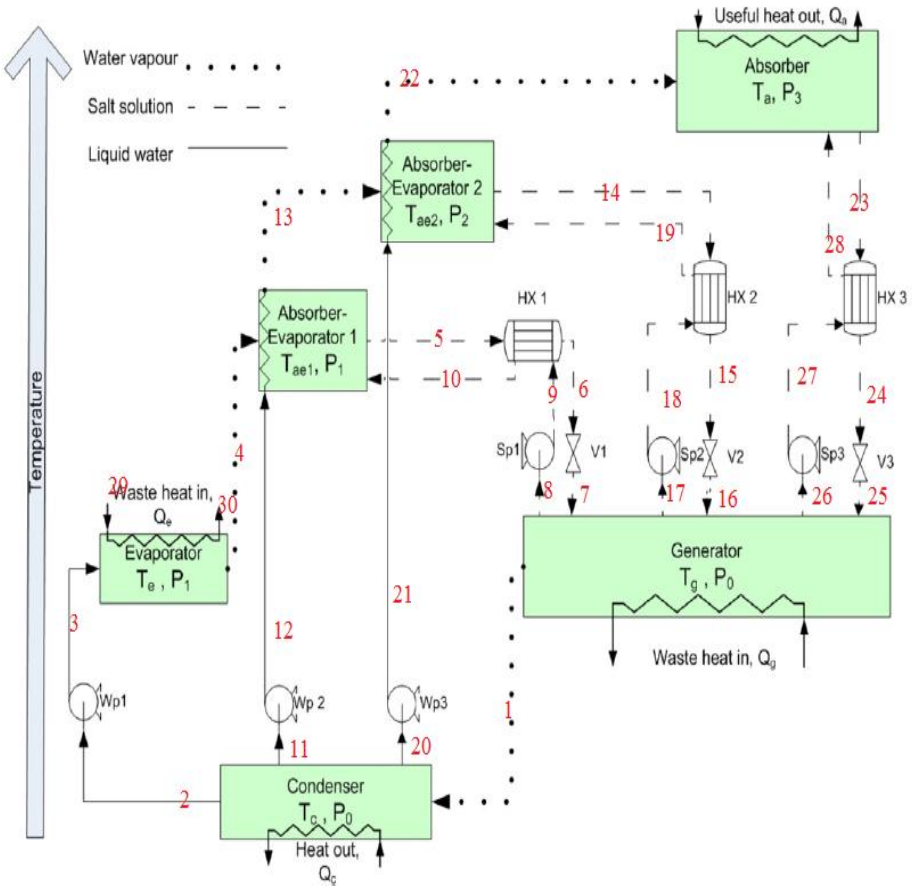

Figure 2.3. Schematic view of conventional triple absorption heat transformer

The 5th case was the best design using four heat exchangers and has an additional heat recovery for the refrigerant vapor exiting condenser prior to absorber/evaporator1. Finally the 6th case has five heat exchangers, four splits and two combos for the aim of increasing the heat recovery of the system which leads to COP increment. In the following chapter the system description and simulation is presented.

Chapter 3

SYSTEM DESCRIPTION AND SIMULATION

3.1 System Description of Conventional TAHT

As mentioned earlier Donnellan et al. [13] introduced six different configurations of a TAHT utilizing H_2O/LiBr as the working pair. Figures 3.1-3.6 display the six alternative designs of TAHTs integrated with desalinations systems.

The third configuration shown in Fig. 3.3, illustrates the conventional triple absorption heat transformer. This conventional TAHT contains a generator, a condenser, an evaporator, an absorber, first absorber/evaporator (AB/EV1), second absorber/evaporator (AB/EV2) and three economizers. The transmitted heat to the evaporator and generator are from the waste hot water of a textile factory. The rejected heat from the absorber provides the thermal energy demanded by the desalination system. Superheated water vapor which works as refrigerant leaves the generator to the condenser where it is condensed to its saturation level. The pressure of the first condensed refrigerant entering to evaporator is increased to the evaporator (P_1) pressure by the first refrigerant pump (RP1). In the evaporator, water is heated to saturated vapor with the waste heat provided to the generator. The vaporized water is absorbed in the AB/EV1 with the strong solution from the generator. A part of the released heat in the absorber is used to retain the AB/with the higher temperature than the evaporator. The pressure of the second part of the condensed refrigerant is increased to a higher pressure level of the evaporator (P_2) via the second refrigerant

pump (RP2) which is higher than that of P_1 and provides heat to the saturated vapor by utilizing the heat of the absorption preserved by AB/EV_1. The vaporized water is absorbed in AB/EV_2 by the strong solution from generator. Absorption heat is partially used to retain the AB/EV_2 at a higher temperature than AB/EV_1 (i.e. 30-60 °C hotter [13]). The final part of the condensed refrigerant is pumped to the highest pressure level (P3) and consequently the water is heated in AB/EV2 to saturated vapor by the retained heat in the AB/EV2. Finally this saturated vapor is absorbed by the strong absorbent-refrigerant and the exothermic reaction in the absorber increases the temperature approximately 30-60 °C than the temperature of solution in the AB/EV2. The released energy which is in heat form is transmitted to salty water as latent and sensible heat in desalination system as shown in Fig. 2.3.

All the weak solutions coming back from AB/EV_1, AB/EV_2 and absorber are used to preheat the corresponding strong solutions from the generator into the HEX1, HEX2 and HEX3.

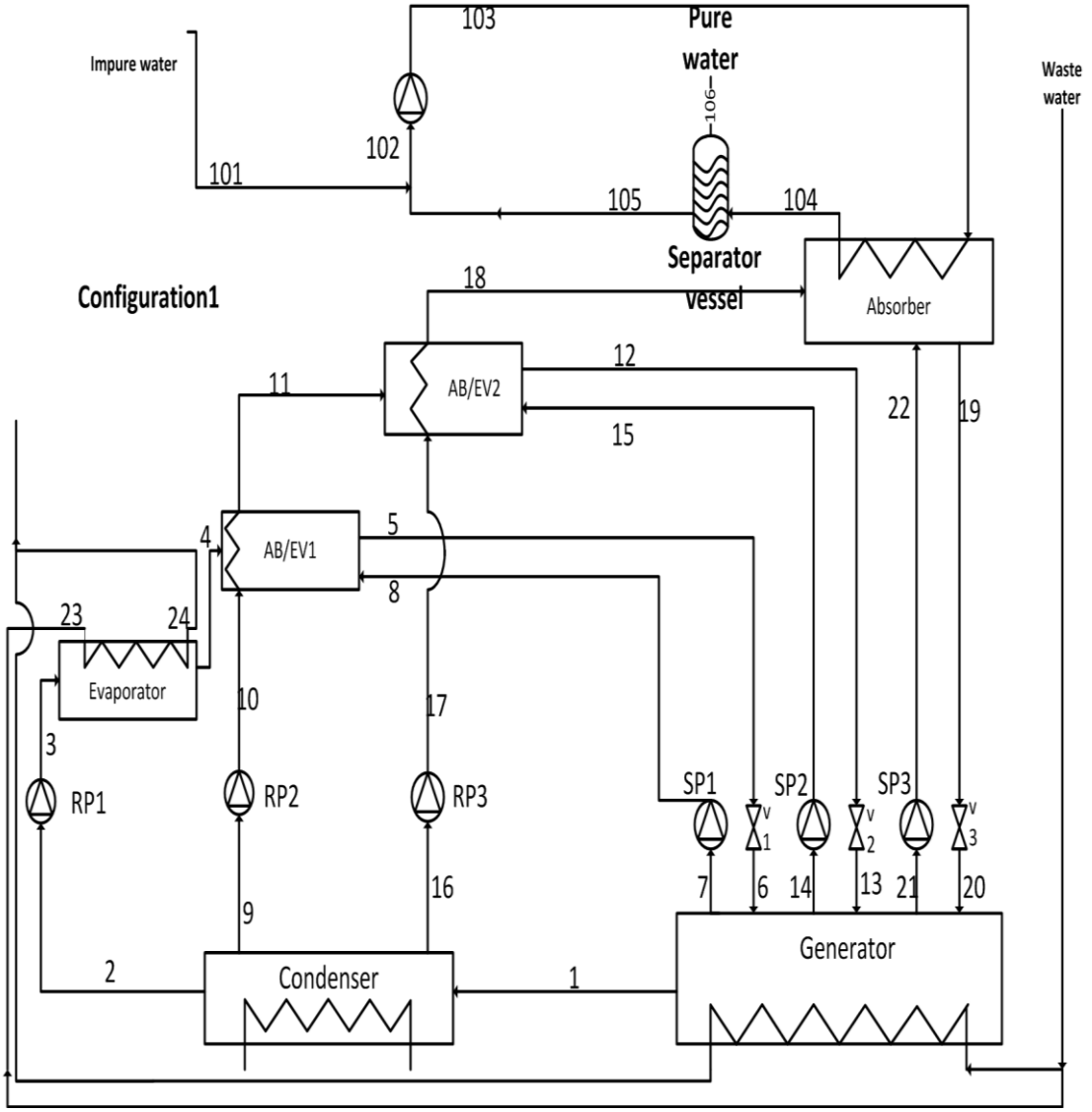

Figure 3.1.Schematic diagrams of seawater desalination system integrated to alternative TAHTs (configuration 1)

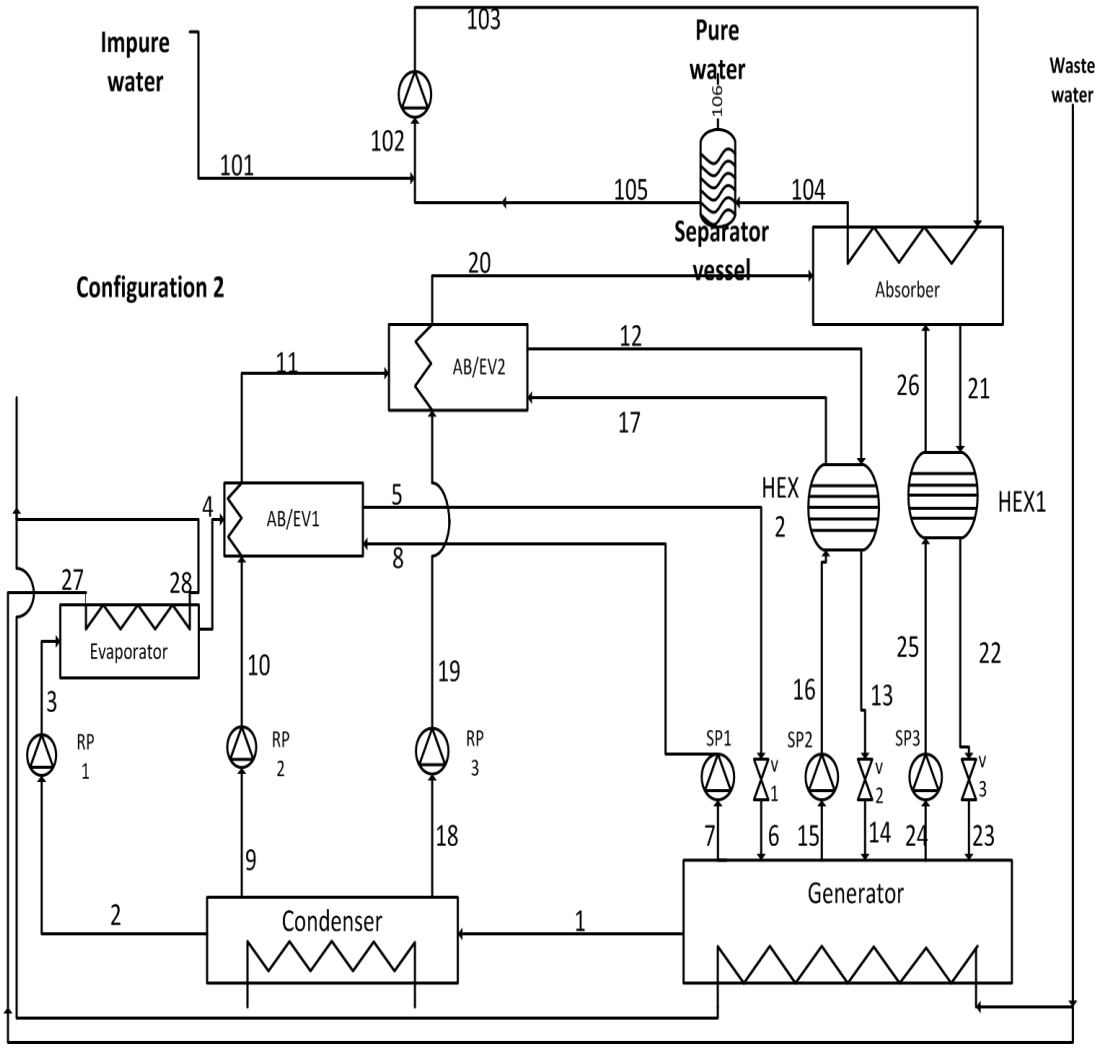

Figure 3.2. Schematic diagrams of seawater desalination system integrated to alternative TAHTs (configuration 2)

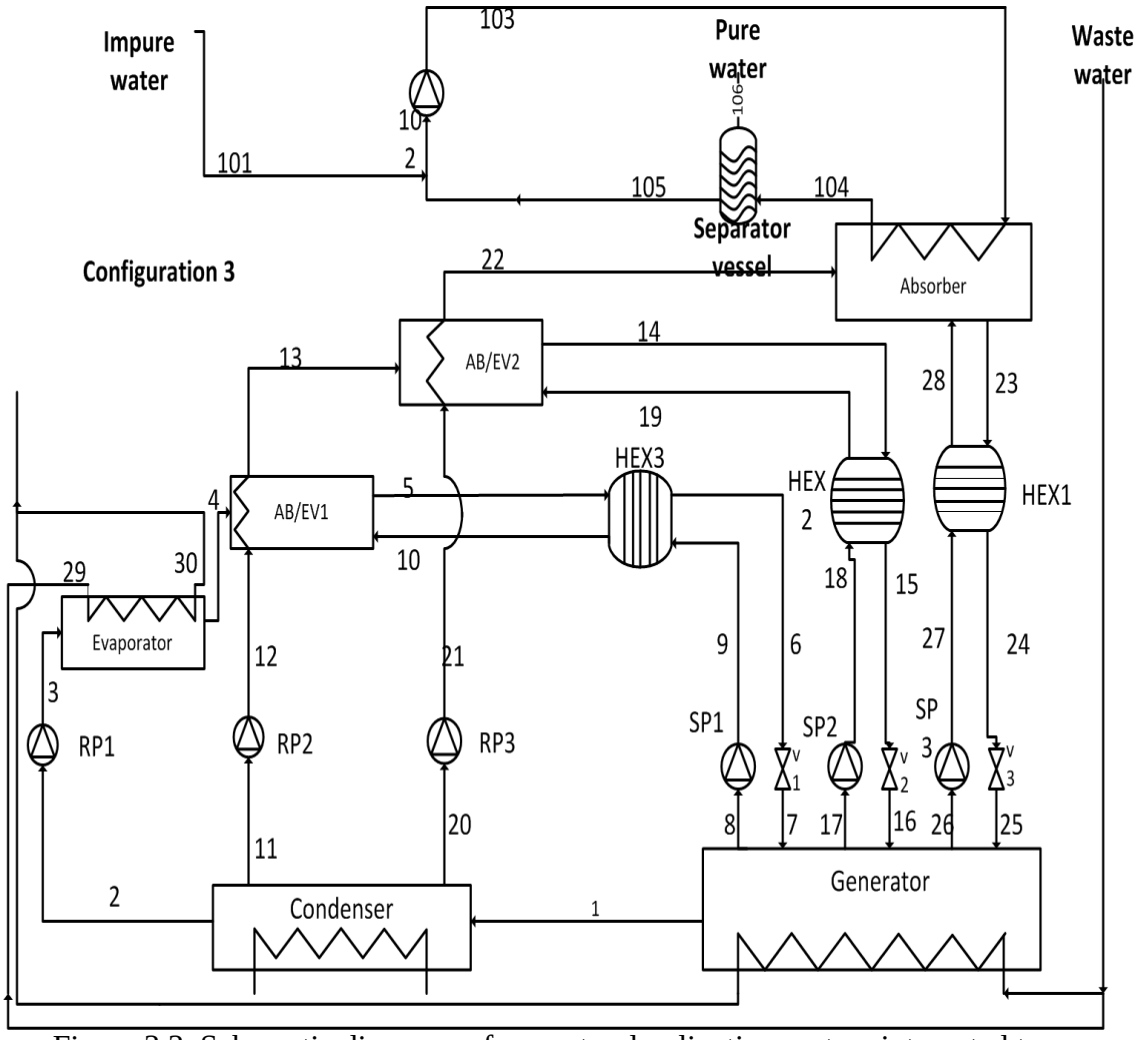

Figure 3.3. Schematic diagrams of seawater desalination system integrated to alternative TAHTs (configuration 3)

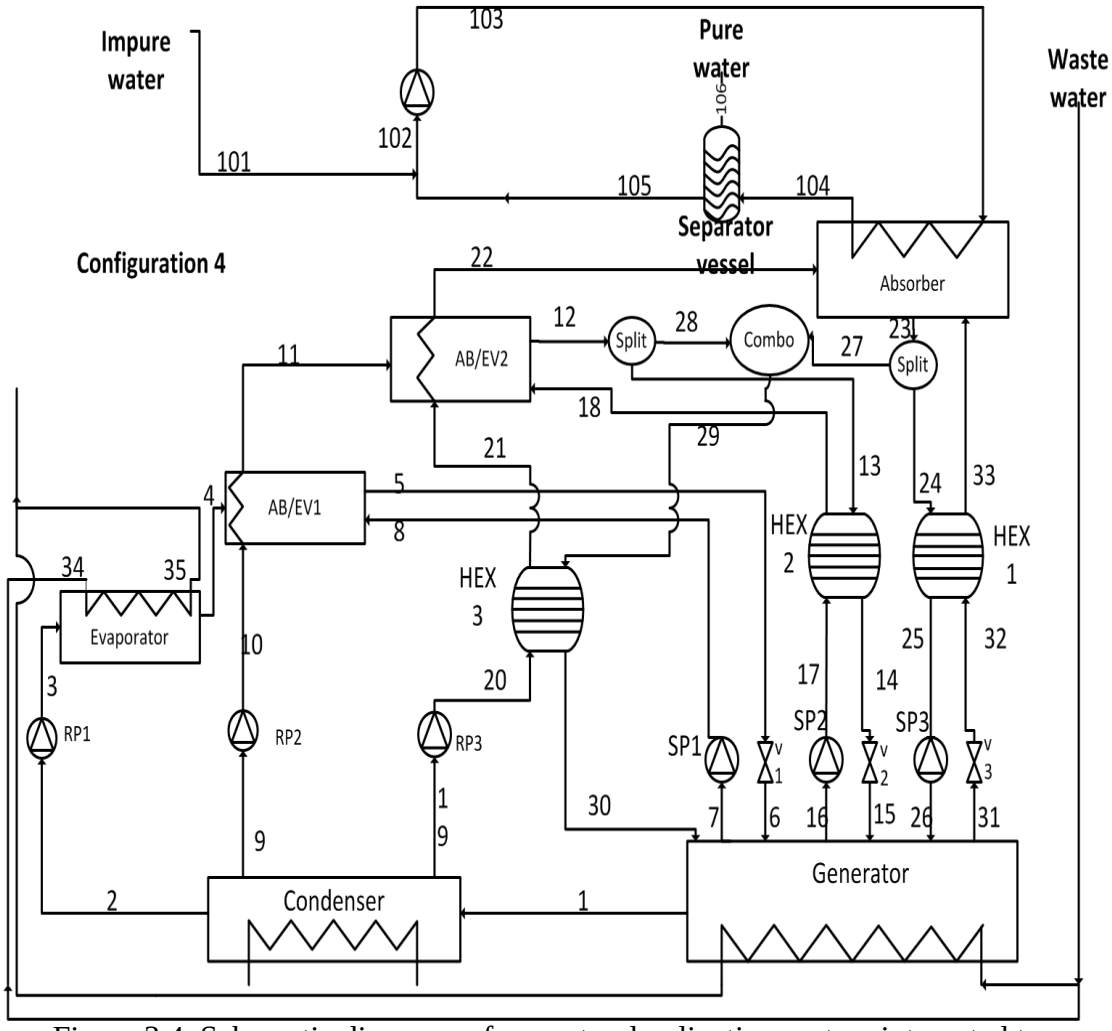

Figure 3.4. Schematic diagrams of seawater desalination system integrated to alternative TAHTs (configuration 4)

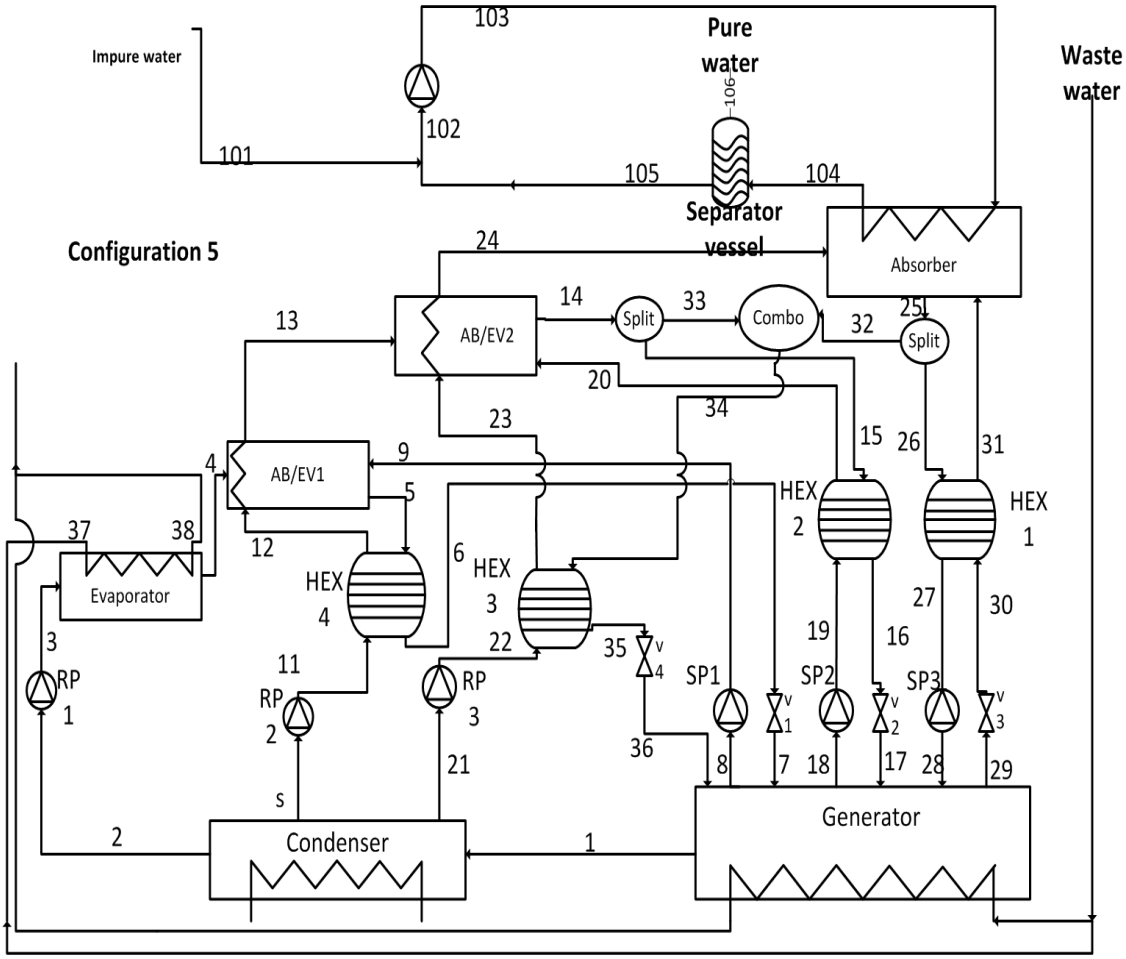

Figure 3.5. Schematic diagrams of seawater desalination system integrated to alternative TAHTs (configuration 5)

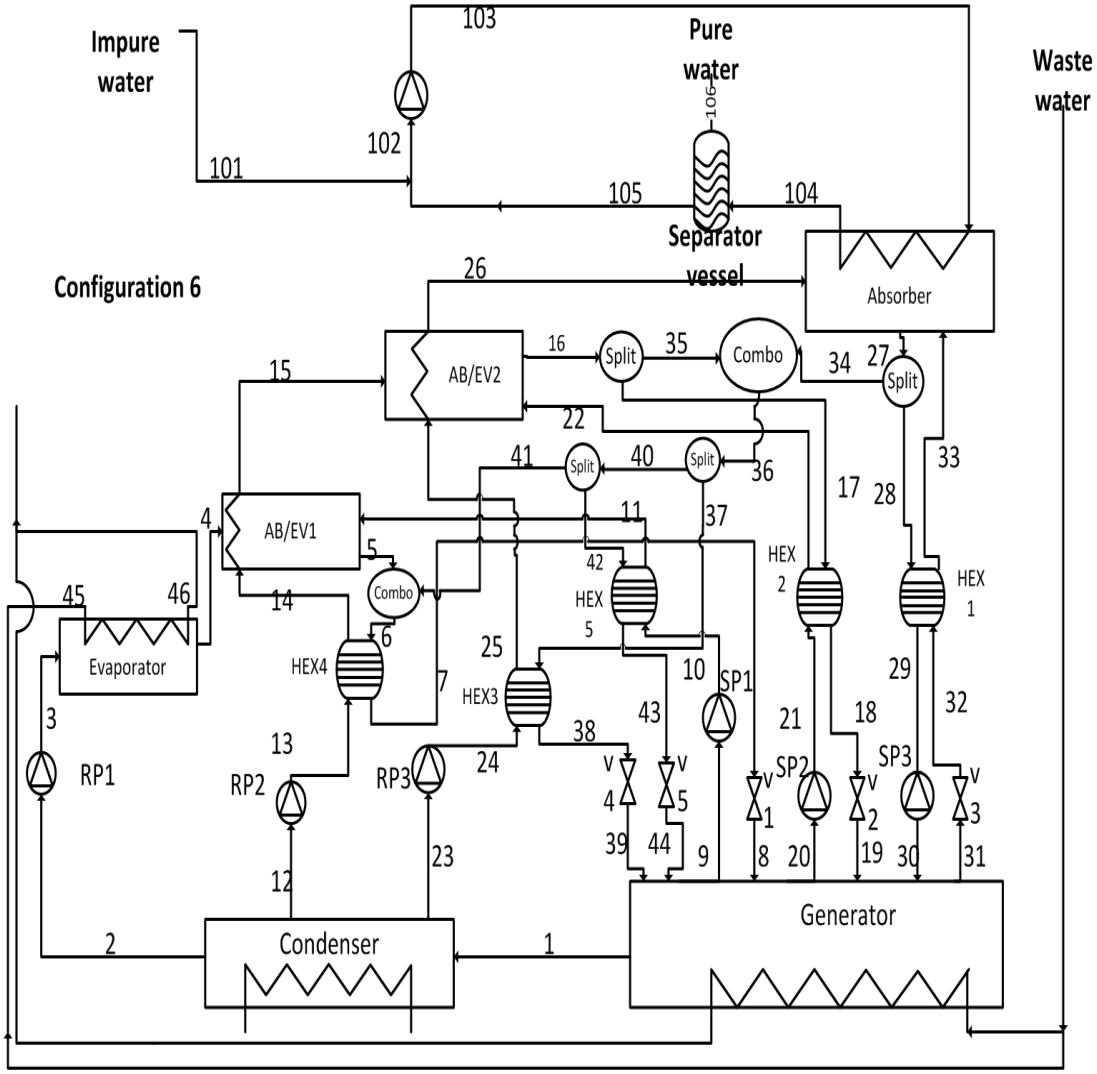

Figure 3.6. Schematic diagrams of seawater desalination system integrated to alternative TAHTs (configuration 6)

3.2 Thermodynamic Modeling

The thermodynamic analyses of the proposed models are explained in the following subsections. The EES software [15] was employed in the simulation of the developed models.

3.3 Assumptions

Simulation was performed by the following assumption:

1. Kinetic and potential energies are constant [13, 17, 20].
2. Components are assumed as control volumes with steady state flow [17].

3. The system is in thermodynamic equilibrium and with the steady flow processes [13, 17, 20, 35].
4. The pressure losses in the connecting pipes are negligible [13, 17, 20, 35].
5. There is no superheating at the exit of the evaporator and there is no sub cooling at the exit of the condenser [13, 17, 20, 35].
6. Heat losses from the main components are not included in the model [13, 20].
7. The salt utilized in the absorbent solution is assumed to have negligible vapor pressure [13, 20].
8. The refrigerant vapor is assumed to evaporate completely in the two absorber-evaporators and the evaporator and condensed completely in the condenser [13, 20]
9. $T_{eva}=T_{gen}$ [13, 20]
10. The supply of the waste heat is from an industrial system of a textile company which has four units with the output of 15 ton/h water at 90 ± 2 °C [9, 17].
11. Pump work is neglected [17].
12. Absorber heat is transferred to impure water as latent and sensible heat [17].
13. The fresh water is salt free [17].
14. The reference temperature for the exergy analysis is $T_o=298.15$ K[13, 20, 35].

3.4 Performance Evaluation

The initial input variables used in simulation processes are presented in Table 3.1.

Table 3.1. The initial input variables in simulation

Parameters	**Value**
T_{con} (°C)	20-35[a]
T_{abs} (°C)	180-215[b]
T_{eva}(°C)	80-90[c]
T_{eva}=T_{gen}(°C)	[d]
$T_{AB/EV1}$(°C)	120-150[e]
$T_{AB/EV2}$(°C)	150-180[f]
$T_{heat\ source}$(°C)	90 ± 2 °C[g]
m heat source (ton/h)	60[g]
ε_{ECO} (%)	80[h]

Where the values are obtained from various studies such as a[37-39]**,** b [13, 20], c[33, 40, 41], d[7, 8, 17, 25, 26], e [13, 20], f[13, 20]**,** g[9, 17].

The system's COP is determined as the ratio of useful heat output systems' over the systems input energy. Due to the fact that COP is the most important criterion of the cycle's capability for upgrading the thermal energy given to system, it is the most important parameter of the cycle. The COP is given in the following equation [13]:

$$COP = \frac{Q\text{abs}}{Qgen+Qeva} \tag{3.1}$$

Where, Q_{abs} is absorber heat capacity (kW), Q_{gen} is generator heat capacity (kW) and Q_{eva} is the evaporator heat capacity (kW).

The magnitude of the useful part of utilized heat for the aim of desalination; $Q_{utilized}$ is a critical parameter [17]:

$$Q_{utilized} = \dot{m}_{104}\,(h_{104}-h_{103}) \tag{3.2}$$

Where $\dot{m}_{104}$ is the mass flow rate of impure water (kg/s) and the h is the specific entalphy of the state 103 and 104 (kj/kg), see Figs 3.1-3.6.

Another fundamental parameter for designing and optimizing the absorption cycles is the flow ratio. It is defined as the ratio of the total mass flow rate of weak solution entering the generator to the mass flow rate of refrigerant vapour leaving the generator [13]:

$$f = \frac{\text{mass flow of salt solution entering the generator}}{\text{mass flow of vapour leaving the generator}} \tag{3.3}$$

The ECOP of the system which deals with the second law of thermodynamics It is defined as the ratio of the maximum useful exergy available from the system to the total exergy entering the system, and it should be maximized as well[13]:

$$\text{ECOP} = \frac{Qabs\left(1-\frac{To}{Tabs}\right)}{Qeva\left(1-\frac{To}{Teva}\right)+Qgen\left(1-\frac{To}{Tgen}\right)} \tag{3.4}$$

Where the To is the ambient temperature (K), T_{eva} is the evaporator temperature, T_{gen} is the generator temperature.

Heat capacities of the main components which defined as the transmitted heat from or to the working fluid for conventional triple absorption heat transformer are presented.

$$Q_{eva=} \dot{m}_{29}(h_{29}-h_{30}) = \dot{m}_{4}(h_4-h_3) \quad (3.5)$$

$$Q_{gen}= \dot{m}_{1}h_1+ \dot{m}_{8}h_8+ \dot{m}_{17}h_{17}+ \dot{m}_{26}h_{26}- \dot{m}_{7}h_7- \dot{m}_{16}h_{16}- \dot{m}_{25}h_{25} \quad (3.6)$$

$$Q_{con}= \dot{m}_{1}h_1- \dot{m}_{2}h_2- \dot{m}_{11}h_{11}- \dot{m}_{20}h_{20} \quad (3.7)$$

$$Q_{abs}=\dot{m}_{22}h_{22}+ \dot{m}_{28}h_{28}- \dot{m}_{23}h_{23} \quad (3.8)$$

$$Q_{AB/EV1}= \dot{m}_{12}(h_{13}-h_{12})= \dot{m}_{4}h_4+ \dot{m}_{10}h_{10}- \dot{m}_{5}h_5 \quad (3.9)$$

$$Q_{AB/EV2}= \dot{m}_{22}(h_{22}-h_{21})= \dot{m}_{13}h_{13}+ \dot{m}_{19}h_{19}- \dot{m}_{14}h_{14} \quad (3.10)$$

3.5 Cycle Optimization

Parametric analyses show that the quantity of the fresh water depends on the temperatures of the generator, evaporator, AB/EV_1, AB/EV_2 and absorber. Therefore the optimum quantity of fresh water output of the system can be expressed as a function of seven design parameters, as shown in the following equation:

$$\text{Maximize } \dot{m}_{distilled_{water}}(T_{gen}, T_{eva}, T_{con}, T_{AB/EV1}, T_{AB/EV2}, T_{abs}) \quad (3.5)$$

Subject to:

$20 \leq T_{con} \leq 35^{o}C$

$80 \leq T_{eva} \leq 90^{o}C$

$80 \leq T_{gen} \leq 90^{o}C$

$110 \leq T_{AB1} \leq 140^{o}C$

$110 \leq T_{EV1} \leq 130^{o}C$

$140 \leq T_{AB2} \leq 180^{o}C$

$140 \leq T_{EV2} \leq 170^{o}C$

$180 \leq T_{abs} \leq 220^{o}C$

The performance of the cycle is optimized by applying the direct search method, assuming the distilled water as the final objective. Direct search method is popular as an unconstrained optimization technique that does not explicitly use derivatives [42].

3.6 Model Validation

A conventional triple absorption heat transformer is basically consisted of a SAHT with additional stages. The available input data for simulating the TAHT were used to simulate SAHT and the model validated by the experimental data presented by Rivera et al. [14]. The assumptions are as follows:

1. Negligible Heat losses and pressure drops in the connecting pipes
2. The flow through the expansion valves is isenthalpic.
3. Economizer effectiveness= 0.7
4. T_{abs}=123 ^{o}C.
5. T_{eva}=T_{gen}= 74.1 °C.

Figure 3 shows the comparison between the COP obtained from the present work with that reported by Rivera et al. [14] . Figure 3 shows that the simulation data is in high coherence with the mentioned experimental data.

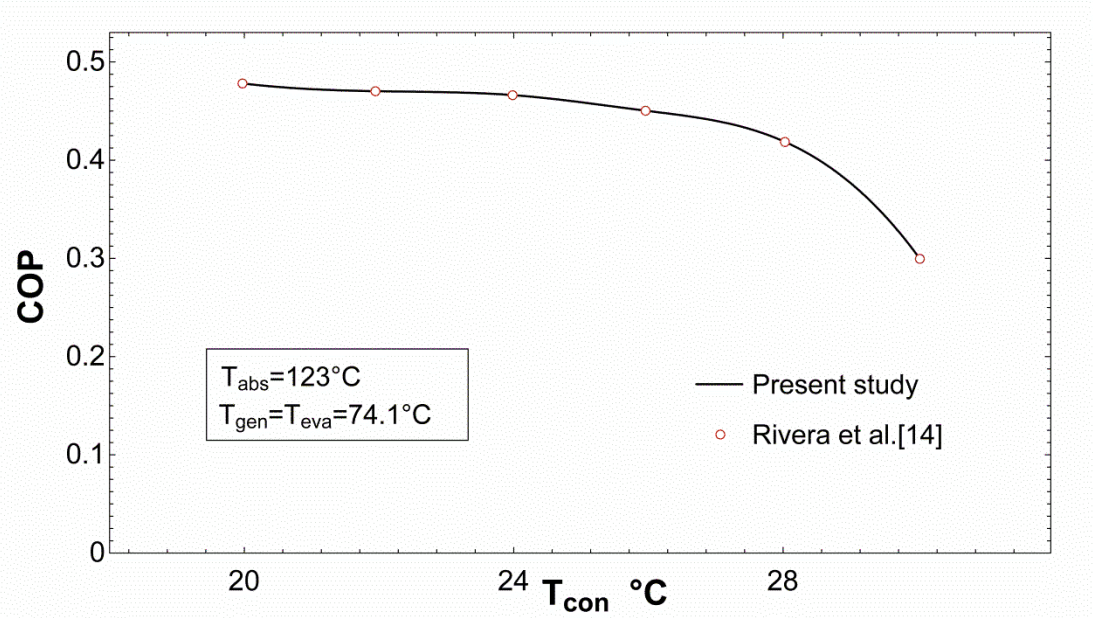

Figure 3.7. Validation of SAHT of the proposed configuration with experimental data

Figure 3.8 and 3.9 show the effect of evaporator temperature on the COP of the conventional system, Fig. 3.8 is obtained from the results of the present study and Fig. 3.9 shows the results from Donnellan et al's work [13].

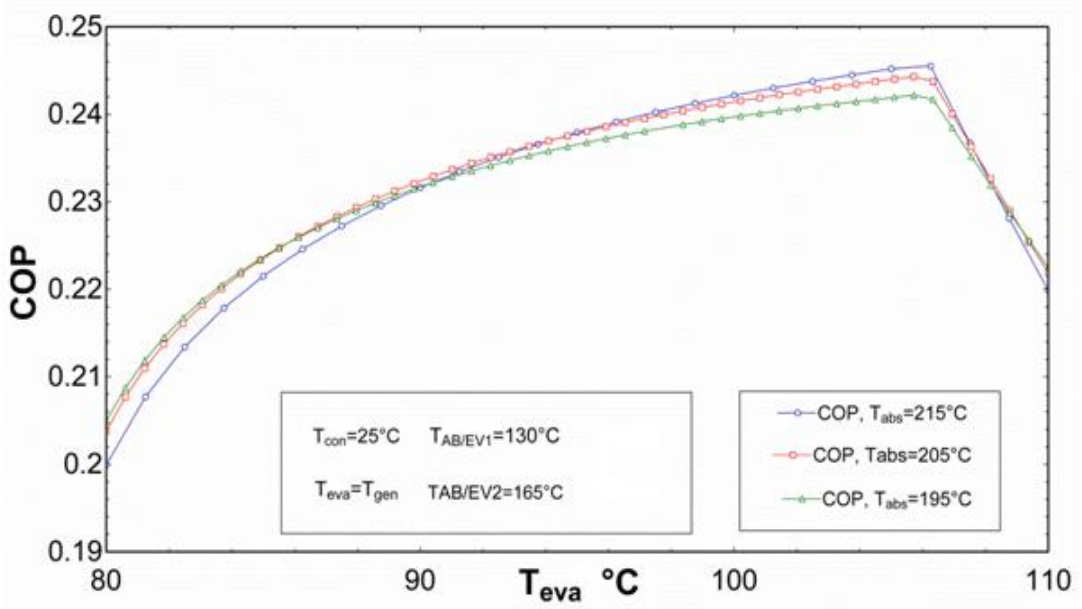

Figure 3.8. Effect of T_{eva} on the COP of the system

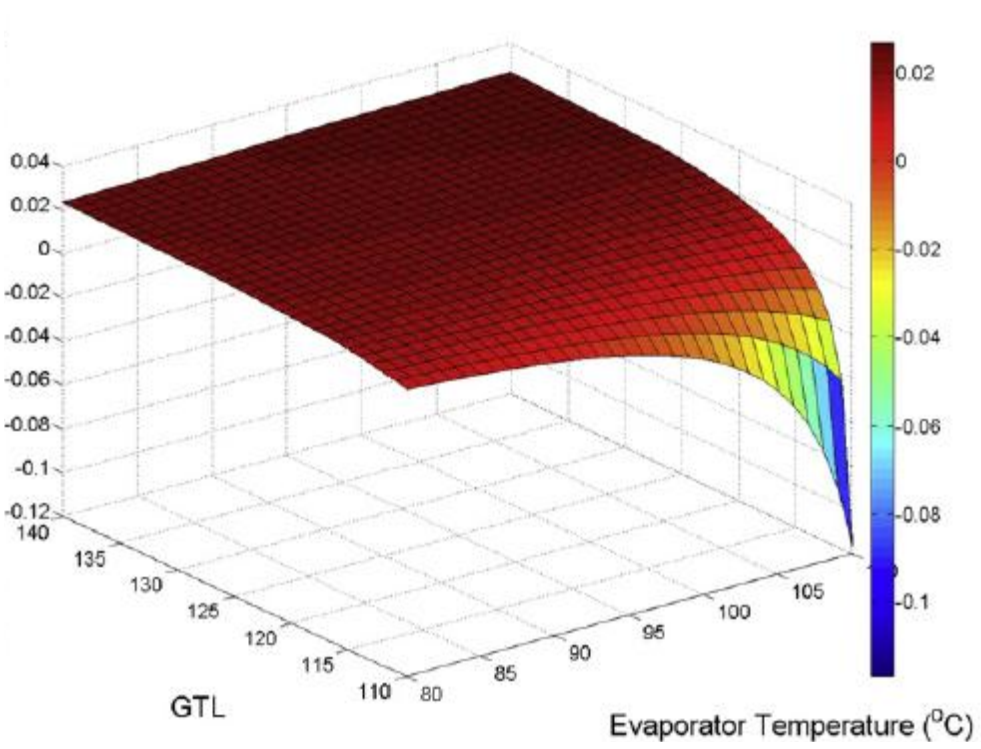

Figure 3.9. Effect of T_{eva} on the COP of the system [13]

The similarity between Fig 3.8 and Fig 3.9 displays the validation of the system. Also the COPs obtained in this study for six configurations are similar to the results of Donnellan et al's study [13]. In order to optimize triple absorption heat transformer Donnllan et al. used both first and second laws of thermodynamics. While the first law is required to determine the energy flows to and from the system, the second law allows for the quantification of irreversibility within the cycle and the identification of sources of loss through the use of an exergy analysis. Also they applied heat exchanger network modeling for optimizing the heat recovery of the systems.

Chapter 4

RESULTS AND DISCUSSION

Results obtained from simulations are presented in this chapter. The impacts of the Tabs on the COP for each configuration for two different Teva are presented in Fig. 4.1. As can be clearly seen in the Fig 4.1, Configuration 1 is more sensible to absorber temperature compared to other configurations and the COP of configuration 6 is nearly constant for all absorber temperatures. For temperatures; T_{con}=25°C, T_{eva}=T_{gen}=80°C, $T_{AB/EV1}$=130°C, $T_{AB/EV2}$=165°C and T_{abs}=215°C the COP of the configuration 6 to 1 are evaluated to be 0.2445, 0.2093, 0.1999, 0.1928, 0.1734, and 0.08926, respectively. By increasing the evaporator temperature to 90°C the COP changed to 0.2513, 0.2401, 0.2316, 0.208, 0.2037 and 0.1467 for configurations 6 to 1 respectively. The COP of the configuration 6 at T_{eva}=90°C is 71.3% and 20.81% more compared to the configurations 1 and 3 respectively. It is obvious that any change in the evaporator temperature has minor effect on the COP of the 6^{th} configuration. For example the change in the COP due to the change in the evaporator temperature from 80 ^{o}C to 90 ^{o}C is about 2.78 % which is much less compared with the other configurations.

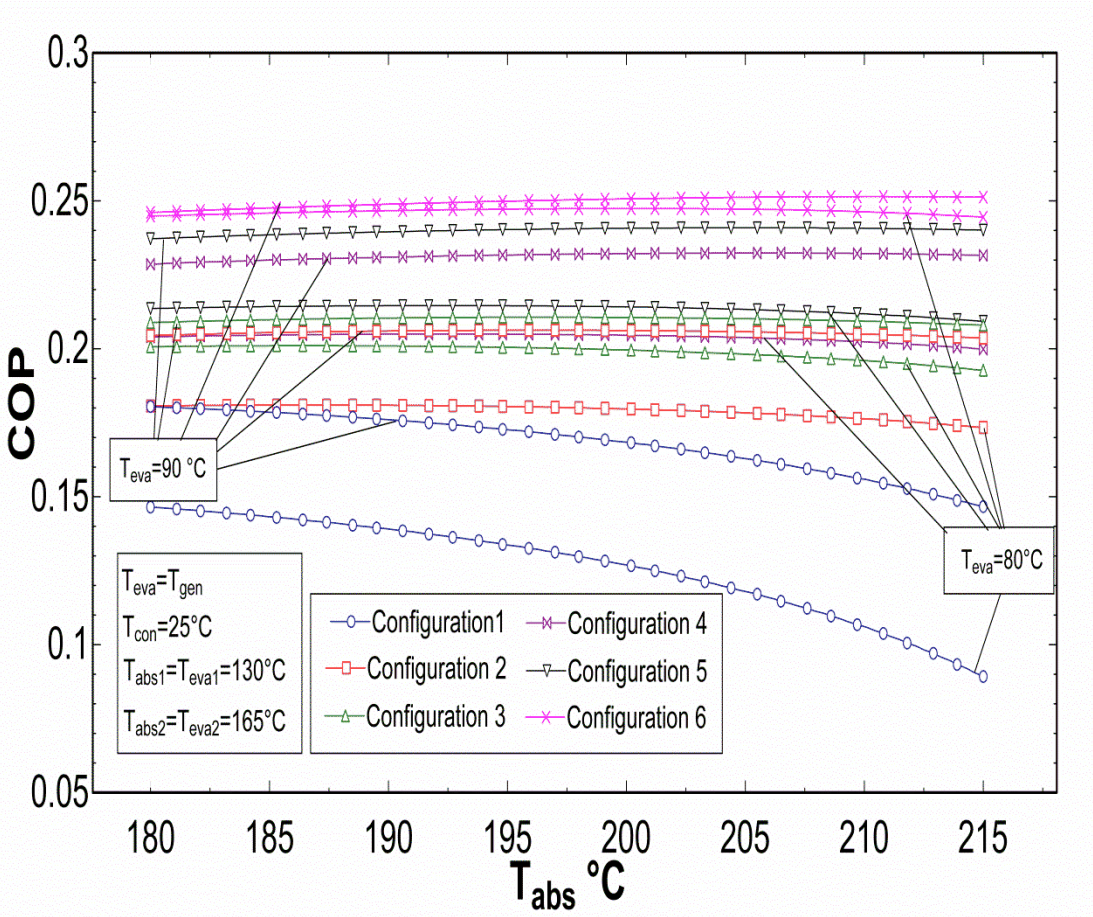

Figure 4.1. Effects of absorber temperature on COP for different configurations at two different evaporation temperatures

The effect of absorber temperature on the utilized heat of the system for the aim of desalination is shown in Fig. 4.2. Once again configuration 6 has the highest utilized heat which is about 323.9kW and 321.5kW with the evaporator temperatures of 90 and 85^{o}C respectively.

It is noticed that by increasing the absorber temperature, COP and Q_u decreases for configurations 1-3 and increases for configurations 4-6 which is also reported in [35]. For configurations 4-6 it seems that the proper assembling of additional heat exchangers are advantageous at higher absorber temperature [13].

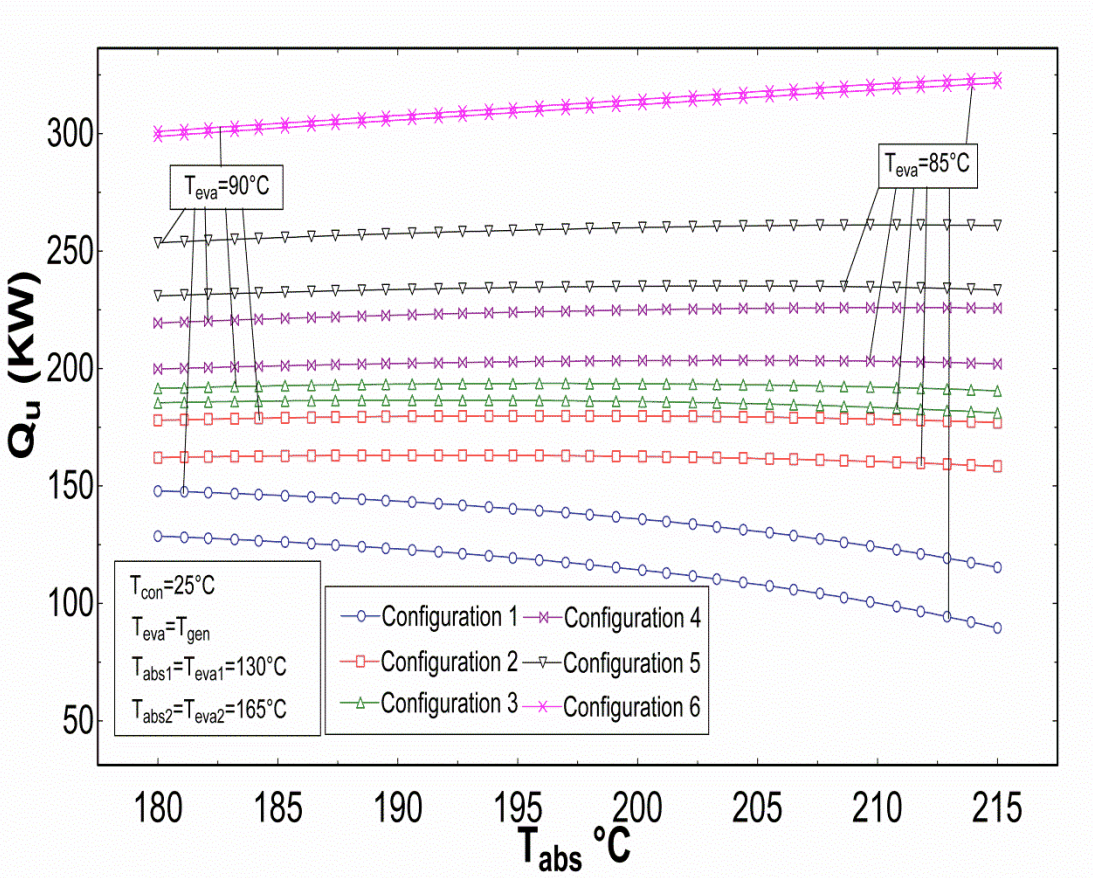

Figure 4.2. Effects of absorber temperature on utilized heat for different configurations at two different evaporation temperatures

The effect of condenser's temperature on the COP of the system is shown in Fig. 4.3. It demonstrates that as the condenser temperature increases, COP of all the configurations are decreasing. It is also observed that the highest COP in all configurations is at T_{con}=20 °C and configuration 6 achieved the highest while configuration 1 has the lowest COP. This is due to the fact that, if the condenser temperature increases, the minimum system pressure will increase and the strong solution concentration will decrease, resulting in an increase of flow ratio. The higher flow ratio will result in the lower absorber heat capacity. This result agrees with that reported in [9, 20].

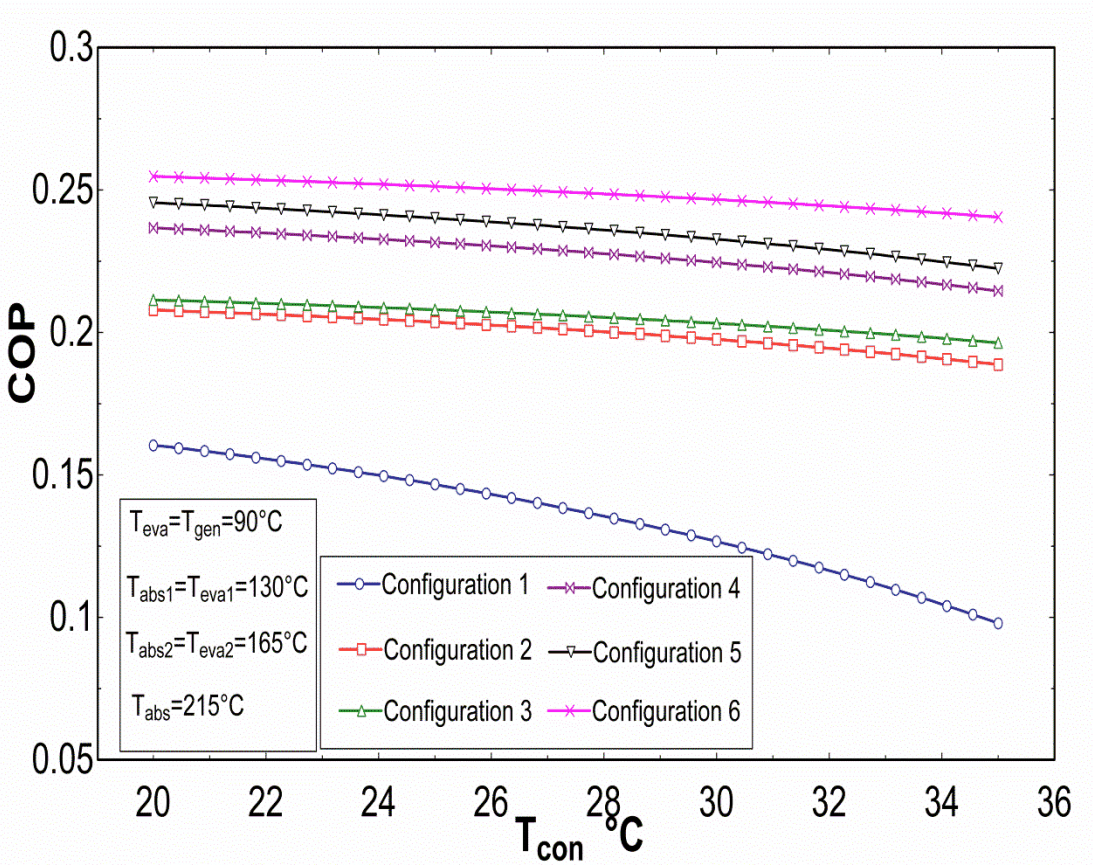

Figure 4.3. Effects of condenser temperature on COP for different configurations

The Pure water production rates were investigated by changing the absorber temperature as shown in Fig. 4.4. The similarity between Figs 4.1, 4.2 and 4.4 is obvious where the amount of utilized heat has indirect relation with increasing T_{abs} for the first three configurations. Similar results have been also reported in [17, 28, 29]. It is clear from the Fig 4.4 that higher water production rate is possible when configuration 6 is employed, which is in coherence with the results indicated in Figs. 4.1 and 4.2. A decline in the distilled mass flow rates is observed when it is progressively moved from configurations 6 to 1.

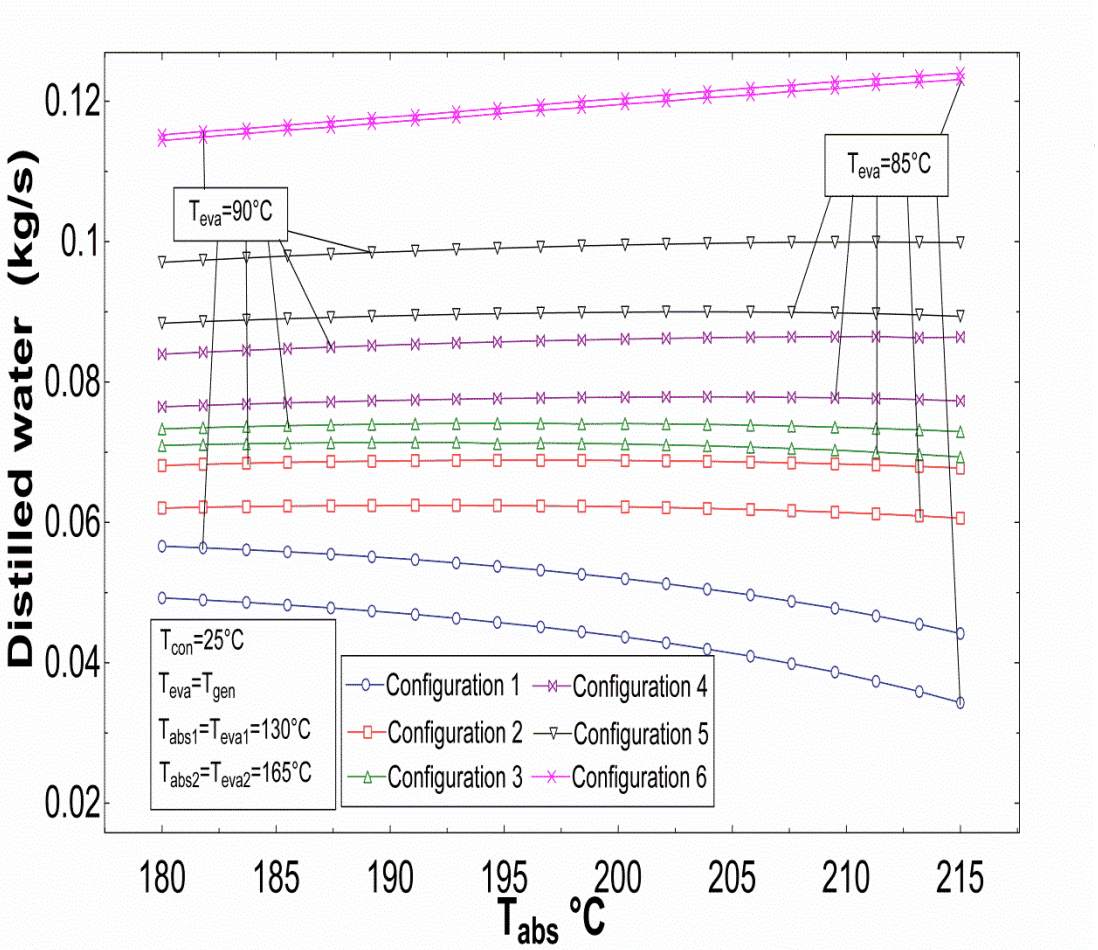

Figure 4.4. Effects of absorber temperature on distilled water for different configurations at two different evaporation temperatures

Concentration of the working pair including LiBr and H_2O in TAHTs are mainly classified in two categories: strong solution (X_s, from the generator to absorber) and weak solution (X_w, from the absorber to the generator). In Fig. 4.5, both the X_s, X_w are plotted against the absorber temperature. It is clear that when generating, condensing and absorber/evaporator temperatures are kept constant, X_s does not vary with T_{abs} but the X_w is increasing. For higher evaporator or generator temperatures, the strong solution is higher. Flow ratio is directly dependent of the X_s which can cause LiBr crystallization problem [9, 17, 28]. Thus, it can be concluded that higher evaporator and generator temperatures enhance the risk of crystallization in the TAHTs.

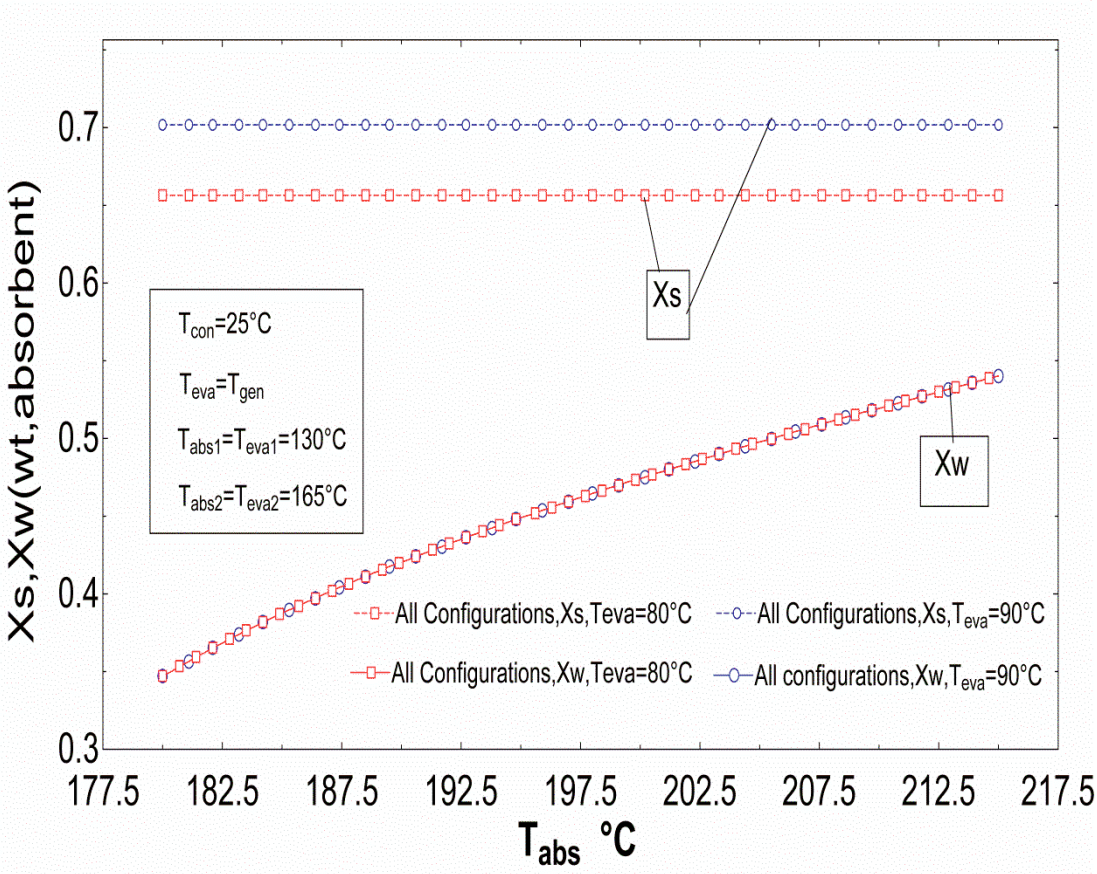

Figure 4.5. Effects of absorber temperatures on Xs and Xw for different configurations at two different evaporation temperatures

The concentration difference ($\Delta X=X_s-X_w$) exhibits a parabolic decrease with increasing absorber temperature as shown in Fig 4.6. As mentioned correspondingly in the literature [17, 28, 43], when T_{gen}, T_{eva}, $T_{AB/EV}$, T_{con} are not varying, the ΔX and T_{abs} are varying as a function of flow ratio (f), which can be easily controlled. Higher f also results in higher T_{abs} and higher mechanical power losses and also higher possibility of working fluid crystallization. It is explicit that the lower evaporator temperature leads to lower ΔX which is a reasonable result according to the mentioned Figure (see Fig 4.5). This is in agreement with the results of Horuz [9] which indicated that an AHT operates better at higher T_{eva}.

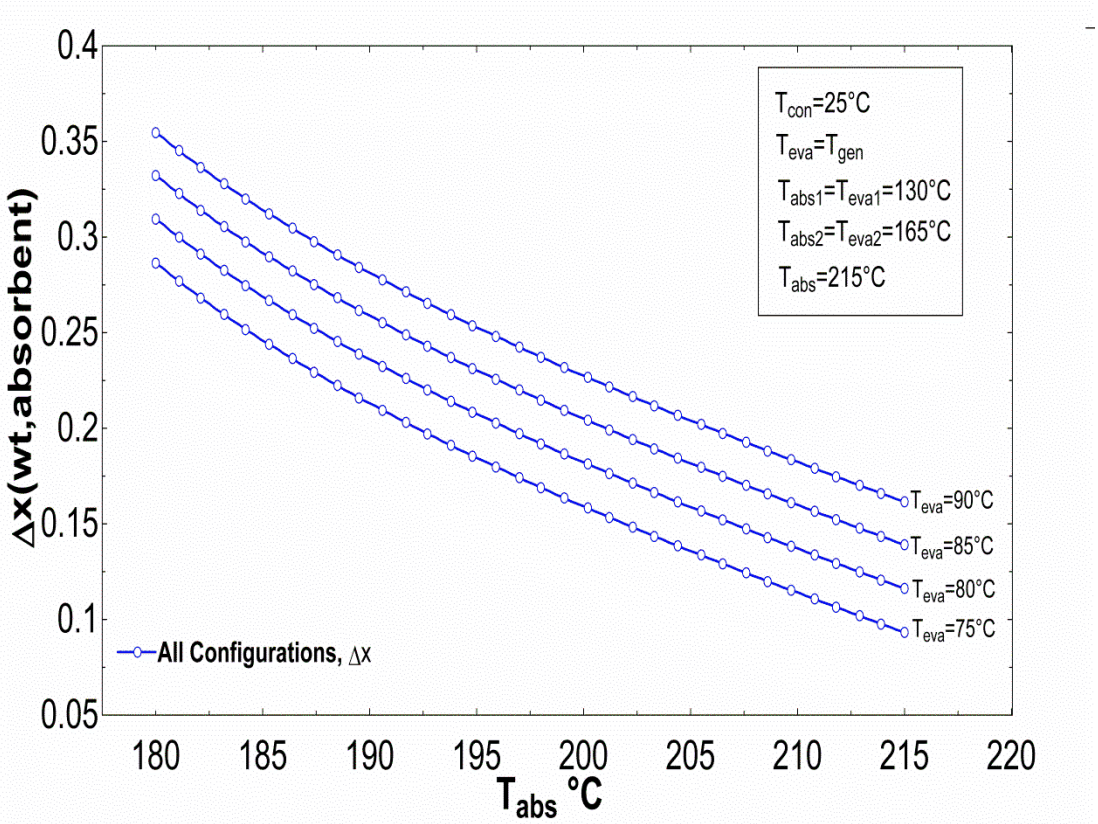

Figure 4.6. Effects of absorber temperature on Δx for different configurations at four different evaporation temperatures

The effects of first GTL ($\Delta T_1=T_{AB1}-T_{gen}$) and second GTL ($\Delta T_2=T_{AB2}-T_{gen}$) on the distilled water and COPs for different configurations are shown in Figs 4.7 and 4.8. The trends of distilled water and COPs are similar. In Fig 4.8 both COP and distilled water production are at maximum in the mid temperature range of AB_2.It can be concluded that the AB_2 temperature should be located at midpoint of highest and lowest possible setting [18, 20].

For all the configurations, the COP and distilled water is almost fixed or decreases moderately by increasing the temperature of the first absorber and second absorber (see Figs 4.7 and 4.8).

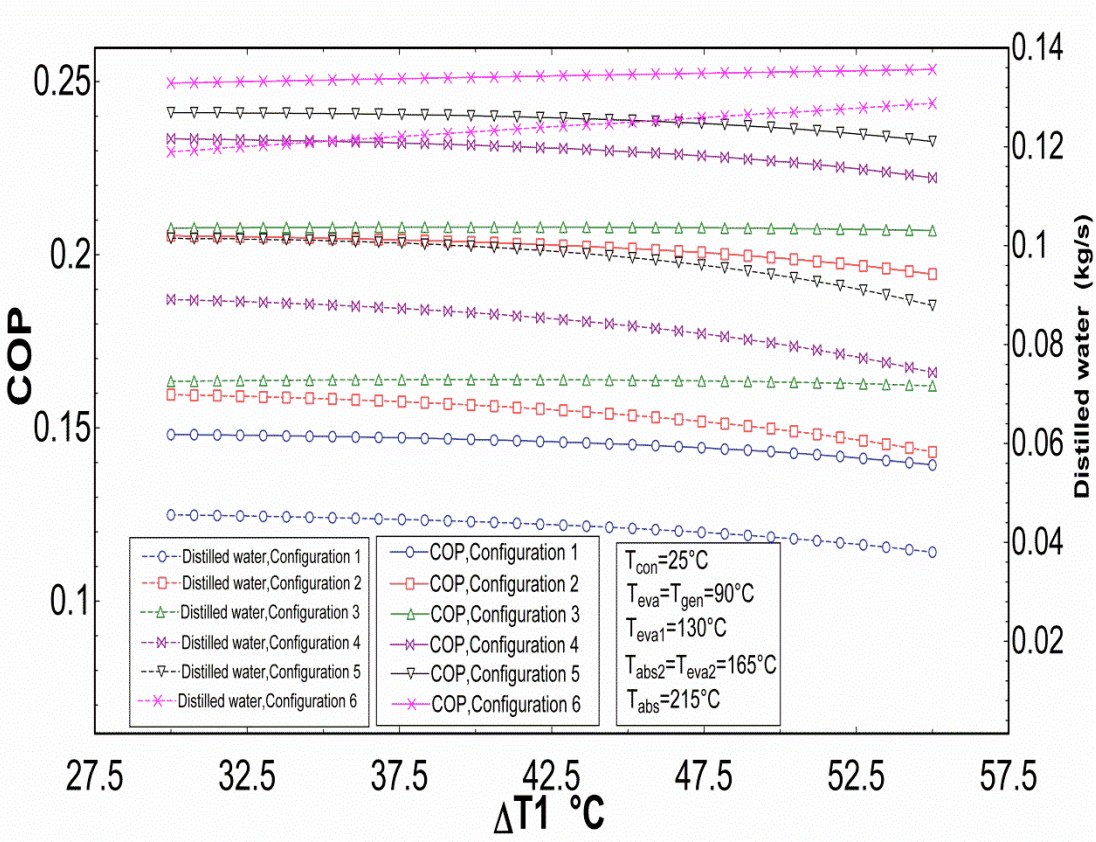

Figure 4.7. Effects of ΔT1 on COP and Distilled water

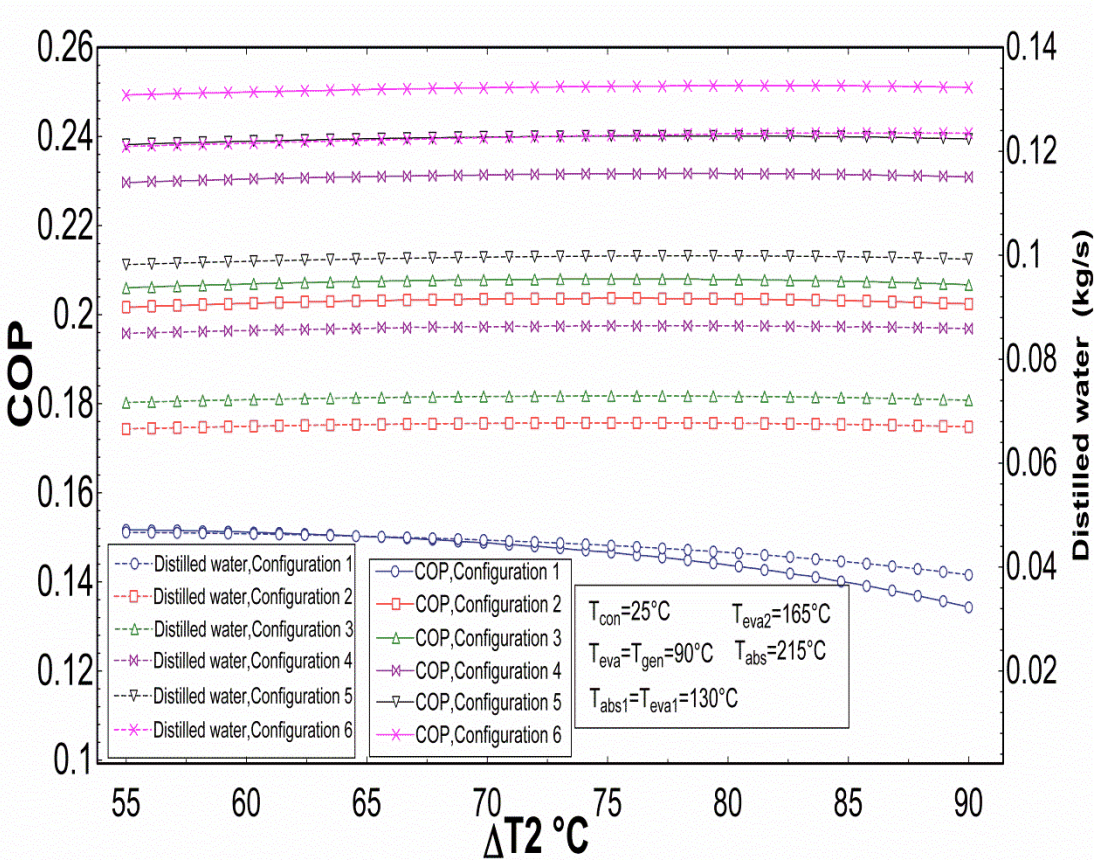

Figure 4.8. Effects of ΔT2 on COP and Distilled water

As explained earlier, performance of the TAHTs depend on several parameters. Utilizing of economizers seems to be absolutely essential for better performance of TAHTs and higher productivity in the case of desalination. The performance of economizer is highly dependent on its effectiveness which is defined for any economizer. As demonstrated in the next two Figures (Fig. 4.9 and Fig 4.10), both the COP and distilled water are dependent on the of economizer effectiveness.

In Fig 4.9 COPs of the six different configurations are depicted versus economizer effectiveness varying from 0.1 to 0.8. Since first configuration does not possess any economizer, COP is taken as constant. As it is clear from the fig. 4.9 the impact on the COPs by utilizing economizer is increased by increasing the economizer effectiveness.

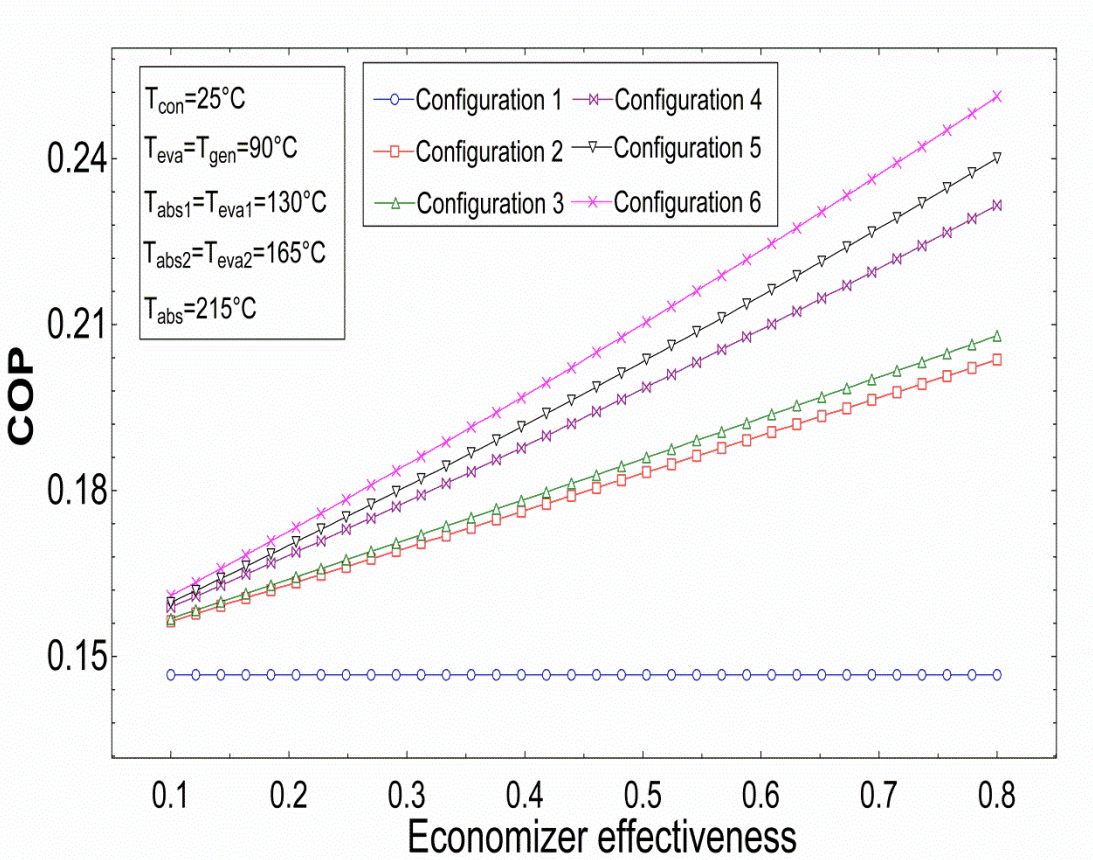

Figure 4.9. Effects of economizer effectiveness on COP for different configurations

Furthermore, the slope of the COPs depend on the number and placement of the economizers. It is evident that configurations 2 and 6 have the lowest and highest slopes respectively.

The rate of water productivity against economizer effectiveness is illustrated in Fig 4.10. It is obvious that, the rate of distilled water highly depends on the economizer effectiveness too. The percentage increase for the configurations 2-6 when heat exchanger effectiveness varies between 0.1 to 0.8 are evaluated to be 41.67%, 51.015%, 75.94%, 99.91%, 145.12%, respectively. The amount of fresh water for configuration 6 is the highest and the lowest for configuration 2 which is an expected result. From the obtained results it can be concluded that the economizer effectiveness should be as high as possible for the highest fresh water yield [35].

The influence of evaporator temperature on the COP is shown in Fig.4.11. It is clear that as the evaporator temperature are increased, the COP of the TAHTs increases slightly. This is due to the fact that, increasing evaporator temperature (and pressure) leads to a lower weak solution concentration and flow ratio (f). The lower flow ratio results in a higher absorption heat capacity and as a higher COP [9, 17, 29].

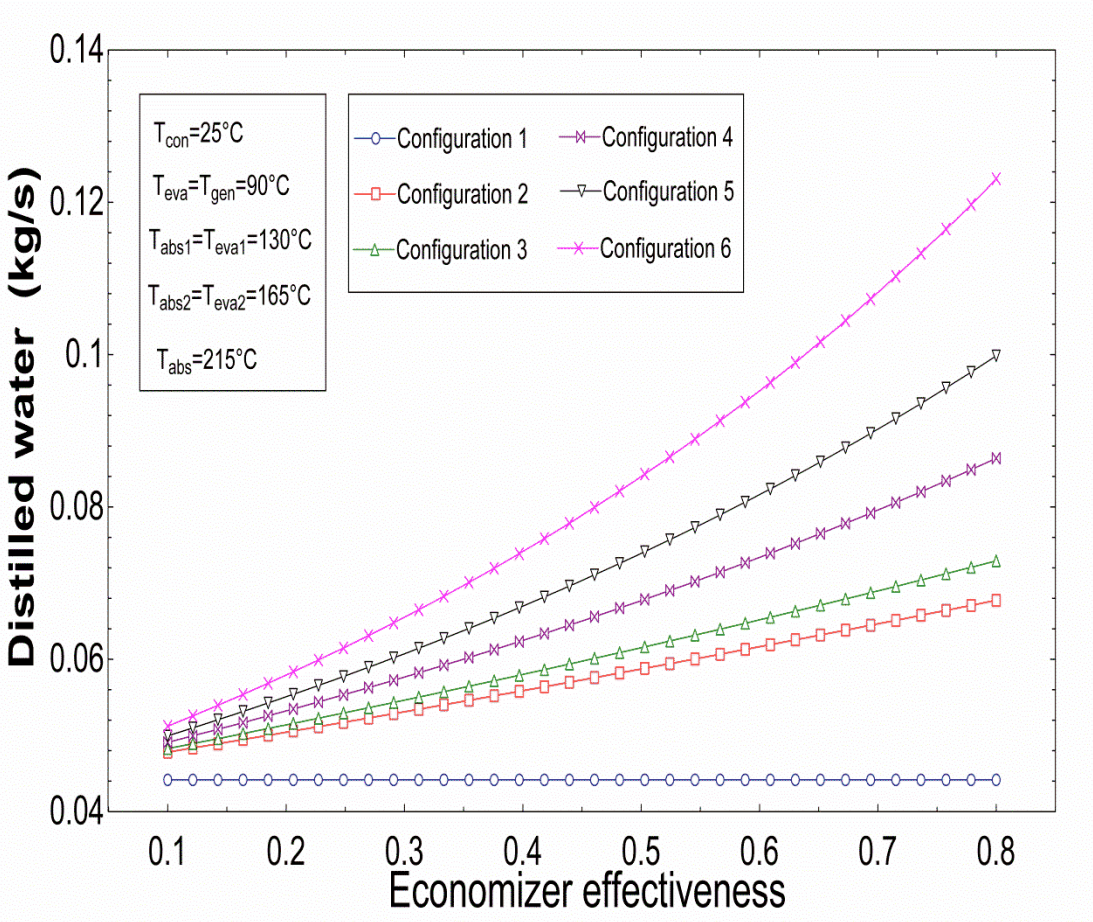

Figure 4.10. Effects of economizer effectiveness on distilled water for different configurations

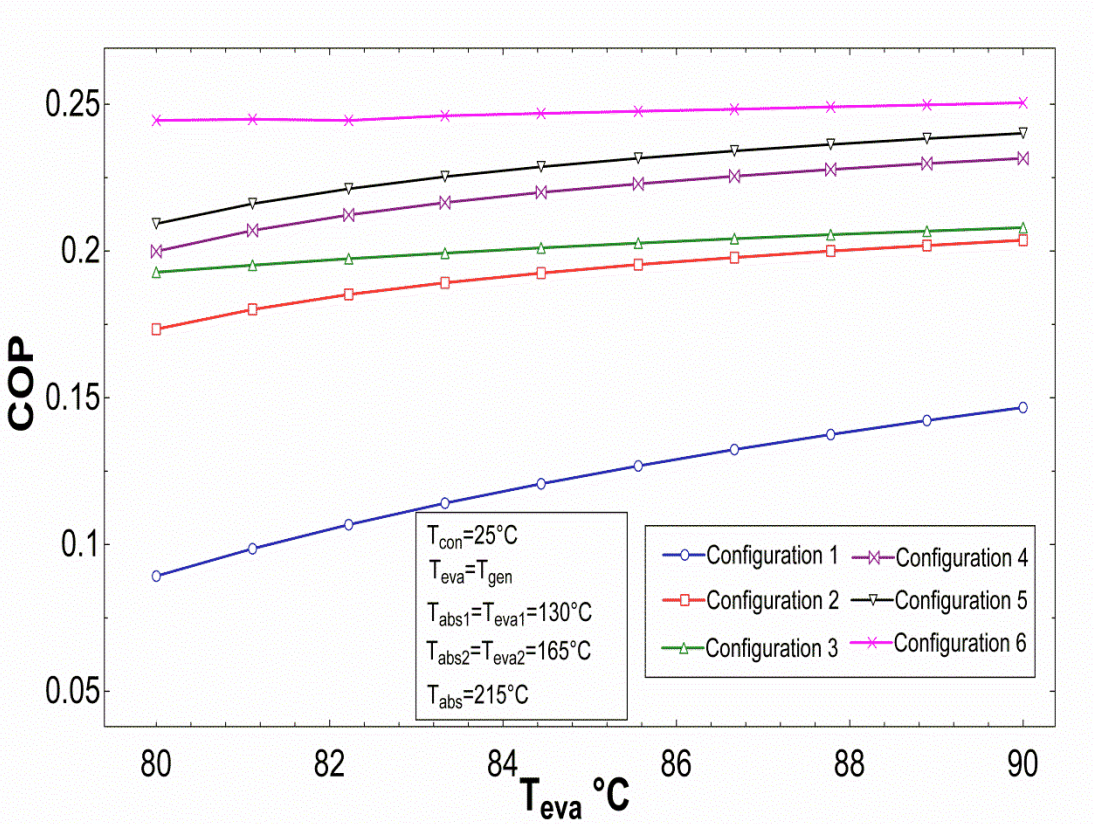

Figure 4.11. Effects of the evaporator temperature on the COP for different configurations

Figure 4.12 shows the variation of ECOP versus absorber temperature. In the first configuration, ECOP decreases slightly as the absorber temperature increased. The main reason is the higher exergy destruction due to the lack of heat exchanger in the first configuration. The maximum of ECOPs for all the configurations are within the range of $200<T_{abs}<215^{o}C$ which corresponds to GTL amount of 110-135.

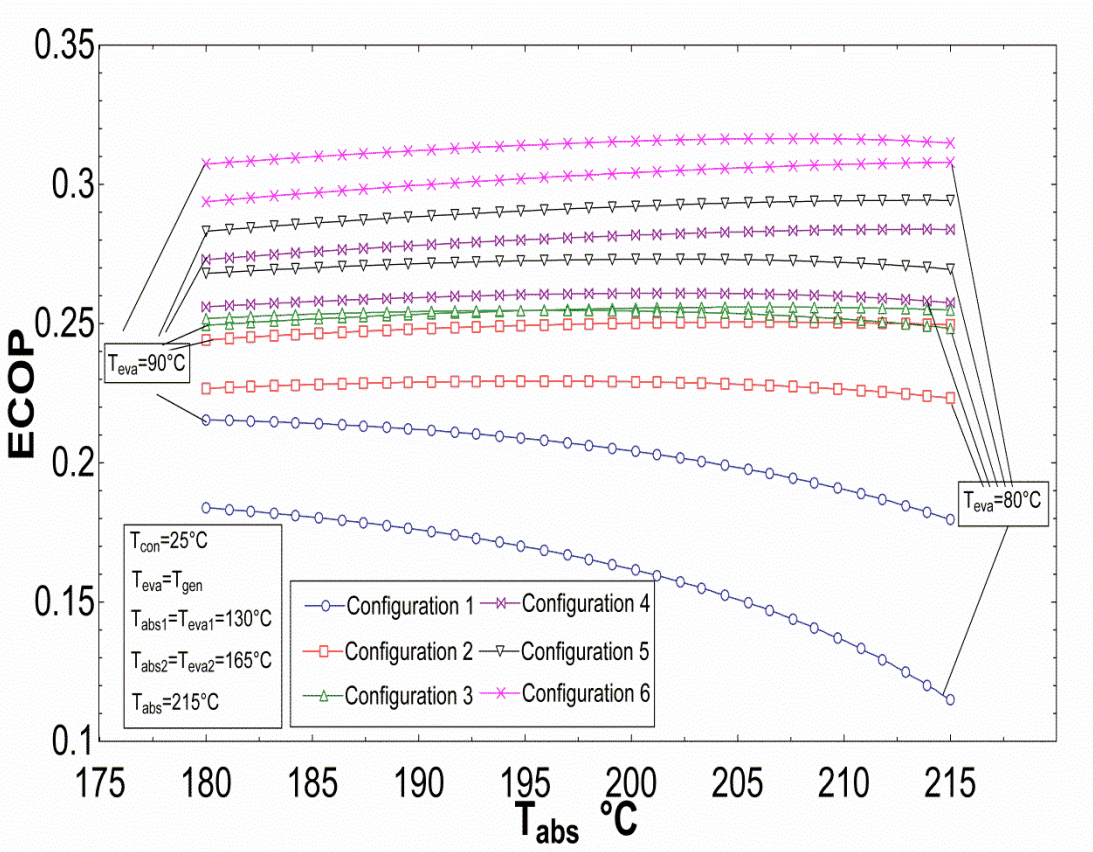

Figure 4.12. Effects of T_abs on ECOP for different configurations at two different evaporator temperatures

As explained earlier (see Figs 4.9, and 4.10), the economizer effectiveness has a major role on the performance of the THAT systems.

Figure 4.13 stresses this consequence from the point of exergetic effectiveness. It is apparent that ECOP of all configurations except configuration 1, (i.e. with no economizer in the cycle) increases sharply as the effectiveness increases.

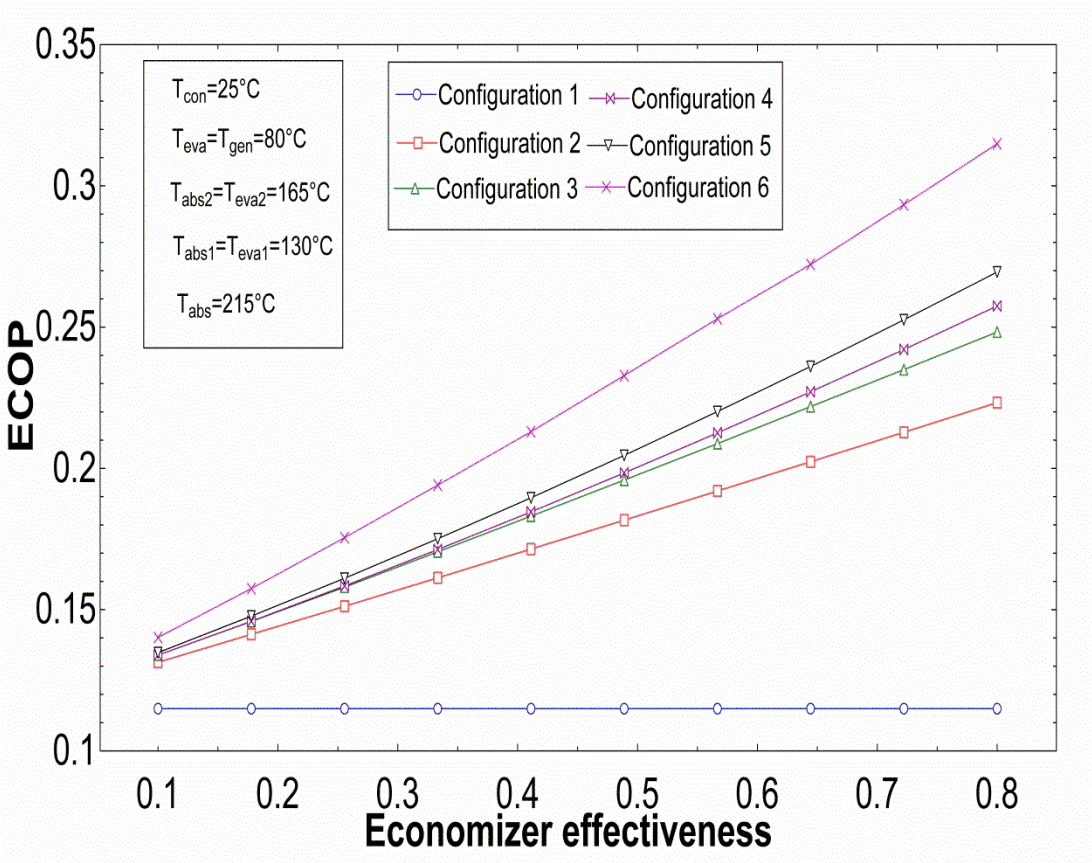

Figure 4.13. Effects of economizer effectiveness on ECOP for different configurations

It is clear from the simulations results that the highest impact on the COP and ECOP for the six configurations (except configuration 1) is due to the economizer effectiveness.

Chapter 5

OPTIMIZATION

5.1 Methodology

The optimization performed by direct search method using EES software. Direct search method is one of the best known iterative optimization techniques that do not use any approximation of gradients. The history of the direct search method arises from 1960s and became very popular in optimization procedures. Direct search method was applied for solving economic and engineering problems[44]. In this study optimization was performed by assuming 6 different constant evaporator temperatures. The objective of the optimization is to finding the maximum fresh water production rate for each configuration. Also the temperatures of the main components are set as constraints. The constraints were explained earlier in chapter 3.

5.2 Optimization Results

The results are summarized in Tables 5.1-5.6 for all configurations where six different evaporator temperatures were assumed.

Table 5.1. Optimization results for Configuration 1

T_eva =T_gen °C	T_con °C	T_eva1 °C	T_abs1 °C	T_eva2 °C	T_abs2 °C	T_abs °C	COP	ECOP	Fresh water(kg/s)
80	20	110	110	140	140	180	0.1723	0.2162	0.05598
82	20	110	110	140	140	180	0.1781	0.221	0.05888
84	20	110	110	140	140	180	0.1833	0.2251	0.6146
86	20	110	110	140	140	180	0.1879	0.2284	0.06374
88	20	110	110	140	140	180	0.1918	0.2311	0.06572
90	20	110	110	140	140	180	0.1953	0.2311	0.06742

Table 5.2. Optimization results for Configuration 2

T_eva =T_gen °C	T_con °C	T_eva1 °C	T_abs1 °C	T_eva2 °C	T_abs2 °C	T_abs °C	COP	ECOP	Fresh water(kg/s)
80	20	104	110	132.2	140	180	0.2169	0.2702	0.07568
82	20	103.8	110	130.1	140	180	0.2197	0.2726	0.07879
84	20	103.5	110	130	141.3	180	0.2222	0.2728	0.08048
86	20	103.2	110	130.2	142.4	180	0.2244	0.2728	0.08193
88	20	102	111	130	142.7	180	0.2265	0.2728	0.08331
90	20	100	113.8	130	142.2	180	0.2286	0.2729	0.08473

Table 5.3. Optimization results for Configuration 3

T_eva =T_gen °C	T_con °C	T_eva1 °C	T_abs1 °C	T_eva2 °C	T_abs2 °C	T_abs °C	COP	ECOP	Fresh water(kg/s)
80	20	100	117.3	132.2	140	180	0.2205	0.2752	0.07987
82	20	100	122.9	130.1	140	180	0.2229	0.2759	0.08137
84	20	100	127.5	130	140	180	0.2252	0.2764	0.08277
86	20	100	128.3	130	140	180	0.226	0.2765	0.08354
88	20	100	135.9	130	140	180	0.229	0.2766	0.08518
90	20	100	137.7	130	143.3	180	0.2305	0.2767	0.08612

Table 5.4.Optimization results for Configuration 4

T_eva =T_gen °C	T_con °C	T_eva1 °C	T_abs1 °C	T_eva2 °C	T_abs2 °C	T_abs °C	COP	ECOP	Fresh water(kg/s)
80	20	118	120	165	165	203.4	0.227	0.2902	0.08372
82	20	116.2	120	165	165	205.3	0.2304	0.2917	0.08703
84	20	114.2	120	165	165	207.4	0.2334	0.2927	0.08983
86	20	112.1	120	165.2	165.2	209.4	0.2359	0.2934	0.09227
88	20	110.8	120	165.1	165.1	212.8	0.2382	0.2941	0.09441
90	20	109.2	120	165.1	165.1	213.5	0.2405	0.294	0.09637

Table 5.5.Optimization results for Configuration 5

T_eva =T_gen °C	T_con °C	T_eva1 °C	T_abs1 °C	T_eva2 °C	T_abs2 °C	T_abs °C	COP	ECOP	Fresh water(kg/s)
80	20	120	120	165	165	200.8	0.2353	0.3003	0.09581
82	20	120	120	165	167.9	204.5	0.238	0.301	0.09887
84	20	120	120	165	167.9	206.7	0.2409	0.302	0.1022
86	20	120	120.2	165	167.9	208.8	0.2435	0.3027	0.105
88	20	118	120	165	167.8	210.6	0.2459	0.3032	0.1075
90	20	115.9	122.4	165	167.7	212.7	0.2481	0.3036	0.1098

Table 5.6. Optimization results for Configuration 6

T_eva =T_gen °C	T_con °C	T_eva1 °C	T_abs1 °C	T_eva2 °C	T_abs2 °C	T_abs °C	COP	ECOP	Fresh water(kg/s)
80	20	120	125.3	165	174	215	0.2452	0.3146	0.1.245
82	20	120	128.1	165	174	215	0.2483	0.3157	0.1263
84	20	121	131.1	165	173	215	0.2516	0.3158	0.1281
86	20	121.1	130.4	165	170	215	0.2534	0.3162	0.1286
88	20	122.5	134.1	165	167	215	0.2554	0.3163	0.1299
90	20	126.2	135.05	165	165	220	0.256	0.3168	0.1307

In all the cases both the COP and fresh water production rate are increasing by rising T_{eva}=T_{gen}. It is obvious that case 1 is completely dependent on the temperatures of evaporator and generator. Among all the cases, configurations 6 represent the best performance followed by configurations 5 to 1 in an ascending order. The maximum value of the optimized COP of the 6^{th} configuration is 0.256 having distilled water production rate of 0.1307 kg/s. The percentage increment of optimized water productivity for configuration 6 compared to other configurations are; 93.85% (case 1), 54.25% (case 2), 51.76% (case 3), 35.62% (case 4) and 19% (case 5).

Based on the results indicated in Tables 5.1-5.6, it can be concluded that the condensation temperature should be kept as low as possible which is in agreement with earlier discussion of Fig. 4.3. As discussed earlier, for the first three configurations the COP and rate of fresh water productivity decreases with increasing the T_{abs}. The trend of COP with evaporator temperature which has been discussed previously in Fig. 4.11 has complete agreement with the results of Tables 5.1-5.6. It can be perceived that both COP and rate of fresh water productivity are increasing by increasing $T_{eva.}$

Jradi et al. [45] demonstrated that each typical residential requires 10 L of fresh water per day. Therefore, assuming that configuration 6 operates non-stop, it will be able to produce enough water for 1131 residential units.

Chapter 6

CONCLUSION

A thermodynamic analysis of TAHT integrated to water desalination system has been conducted for six different configurations using LiBr/H_2O as the working fluid. This study aims to identify the variation of the main parameters such as temperatures of the main components and economizer effectiveness on the performance of the systems. Also, an optimization was made in EES by assuming maximization the quantity of the distilled water as the objective function. Based on the results of the analysis and optimization, following conclusions are drawn:

- The lower the condensing temperature is, the higher the COP will be.
- Higher evaporator and generator temperatures enhance the risk of crystallization in TAHTs.
- The proper assembling of additional HEX, improved the cycle performance of the last three configurations. This means that they were more effective in terms of absorber temperature increment which is a major advantage for the whole cycle.
- The economizer effectiveness should be as high as possible in order to increase significantly the COP, ECOP and the distilled water productivity.
- Configuration 6 has the highest COP value around 30% compared to the first configuration which has the lowest COPamong the six configurations.
- The quantity of pure water production rate increased from configuration 1 to 6

- As the evaporator and generator temperature increased, the COPs for all configurations are also increased
- Configuration 6 is capable of producing fresh water for 1131 residual units.

REFERENCES

1. Ali, M.T., H.E.S. Fath, and P.R. Armstrong, *A comprehensive techno-economical review of indirect solar desalination.* Renewable & Sustainable Energy Reviews, 2011. **15**(8): p. 4187-4199.

2. El-Ghonemy, A.M.K., *Future sustainable water desalination technologies for the Saudi Arabia: A review.* Renewable & Sustainable Energy Reviews, 2012. **16**(9): p. 6566-6597.

3. Aybar, H.Ş., F. Egelioğlu, and U. Atikol, *An experimental study on an inclined solar water distillation system.* Desalination, 2005. **180**(1-3): p. 285-289.

4. Liu, G.Y., et al., *A controlled thermal solar desalination system*, 2014. p. 1529-1532.

5. Goosen, M., H. Mahmoudi, and N. Ghaffour, *Water Desalination using geothermal energy.* Energies, 2010. **3**(8): p. 1423-1442.

6. Yan, X., et al., *Study of an incrementally loaded multistage flash desalination system for optimum use of sensible waste heat from nuclear power plant.* International Journal of Energy Research, 2012.

7. Gomri, R., *Energy and exergy analyses of seawater desalination system integrated in a solar heat transformer*. Desalination, 2009. **249**(1): p. 188-196.

8. Gomri, R., *Thermal seawater desalination: Possibilities of using single effect and double effect absorption heat transformer systems.* Desalination, 2010. **253**(1-3): p. 112-118.

9. Horuz, I. and B. Kurt, *Absorption heat transformers and an industrial application.* Renewable Energy, 2010. **35**(10): p. 2175-2181.

10. Li, M., et al., *Thermo-economic analysis and comparison of a CO2 transcritical power cycle and an organic Rankine cycle.* Geothermics, 2014. **50**: p. 101-111.

11. Guo, C., et al., *Performance analysis of organic Rankine cycle based on location of heat transfer pinch point in evaporator.* Applied Thermal Engineering, 2014. **62**(1): p. 176-186.

12. Yin, J., et al., *Performance analysis of an absorption heat transformer with different working fluid combinations.* Applied Energy, 2000. **67**(3): p. 281-292.

13. Donnellan, P., E. Byrne, and K. Cronin, *Internal energy and exergy recovery in high temperature application absorption heat transformers.* Applied Thermal Engineering, 2013. **56**(1-2): p. 1-10.

14. Rivera, W., et al., *Single stage and double absorption heat transformers used to recover energy in a distillation column of butane and pentane.* International Journal of Energy Research, 2003. **27**(14): p. 1279-1292.

15. Klein, S.A. and F. Alvarado, *Engineering Equation Solver, version 9.237, F-Chart Software.* Middleton 2012.

16. Horuz, I. and B. Kurt, *Single stage and double absorption heat transformers in an industrial application.* International Journal of Energy Research, 2009. **33**(9): p. 787-798.

17. Parham, K., M. Yari, and U. Atikol, *Alternative absorption heat transformer configurations integrated with water desalination system.* Desalination, 2013. **328**: p. 74-82.

18. Zhao, Z., Y. Ma, and J. Chen, *Thermodynamic performance of a new type of double absorption heat transformer.* Applied Thermal Engineering, 2003. **23**(18): p. 2407-2414.

19. Zhao, Z., et al., *The thermodynamic performance of a new solution cycle in double absorption heat transformer using water/lithium bromide as the working fluids.* International Journal of Refrigeration, 2003. **26**(3): p. 315-320.

20. Donnellan, P., et al., *First and second law multidimensional analysis of a triple absorption heat transformer (TAHT).* Applied Energy, 2014. **113**: p. 141-151.

21. Huicochea, A., et al., *A novel cogeneration system: A proton exchange membrane fuel cell coupled to a heat transformer.* Applied Thermal Engineering, 2013. **50**(2): p. 1530-1535.

22. Sekar, S. and R. Saravanan, *Experimental studies on absorption heat transformer coupled distillation system.* Desalination, 2011. **274**(1-3): p. 292-301.

23. Escobar, R.F., et al., *On-line indirect measures estimation for the performance of an absorption heat transformer integrated to a water purification process.* Measurement: Journal of the International Measurement Confederation, 2009. **42**(3): p. 464-473.

24. Hernández, J.A., et al., *A neural network approach and thermodynamic model of waste energy recovery in a heat transformer in a water purification process.* Desalination, 2009. **243**(1-3): p. 273-285.

25. Siqueiros, J. and R.J. Romero, *Increase of COP for heat transformer in water purification systems. Part I - Increasing heat source temperature.* Applied Thermal Engineering, 2007. **27**(5-6): p. 1043-1053.

26. Romero, R.J., J. Siqueiros, and A. Huicochea, *Increase of COP for heat transformer in water purification systems. Part II - Without increasing heat source temperature.* Applied Thermal Engineering, 2007. **27**(5-6): p. 1054-1061.

27. Sözen, A. and H.S. Yücesu, *Performance improvement of absorption heat transformer.* Renewable Energy, 2007. **32**(2): p. 267-284.

28. Zare, V., M. Yari, and S.M.S. Mahmoudi, *Proposal and analysis of a new combined cogeneration system based on the GT-MHR cycle.* Desalination, 2012. **286**: p. 417-428.

29. Yari, M., *A novel cogeneration cycle based on a recompression supercritical carbon dioxide cycle for waste heat recovery in nuclear power plants.* International Journal of Exergy, 2012. **10**(3): p. 346-364.

30. Sun, J., L. Fu, and S. Zhang, *A review of working fluids of absorption cycles.* Renewable and Sustainable Energy Reviews, 2012. **16**(4): p. 1899-1906.

31. Khamooshi, M., K. Parham, and U. Atikol, *Overview of ionic liquids used as working fluids in absorption cycles.* Advances in Mechanical Engineering, 2013. **2013**.

32. Bourouis, A., et al., *Purification of seawater using absorption heat transformers with water-(LiBr+-LiI+LNO3+LiCl) and low temperature heat sources.* Desalination, 2004. **166**(1-3): p. 209-214.

33. Zhang, X. and D. Hu, *Performance analysis of the single-stage absorption heat transformer using a new working pair composed of ionic liquid and water*. Applied Thermal Engineering, 2012. **37**: p. 129-135.

34. Horuz, I., *A comparison between ammonia-water and water-lithium bromide solutions in vapor absorption refrigeration systems.* International Communications in Heat and Mass Transfer, 1998. **25**(5): p. 711-721.

35. Martínez, H. and W. Rivera, *Energy and exergy analysis of a double absorption heat transformer operating with water/lithium bromide.* International Journal of Energy Research, 2009. **33**(7): p. 662-674.

36. Barragán Reyes, R.M., V.M.A. Gómez, and A. García-Gutiérrez, *Performance modelling of single and double absorption heat transformers.* Current Applied Physics, 2010. **10**(2 SUPPL.): p. S244-S248.

37. Best, R. and W. Rivera, *Thermodynamic design-data for absorption heat transformer .6. operating on water carrol*. Heat Recovery Systems & Chp, 1994. **14**(4): p. 427-436.

38. Eisa, M.A.R., R. Best, and F.A. Holland, *Thermodynamic design-data for absorption heat transformer .2. operating on water-calcium chloride.* Journal of Heat Recovery Systems, 1986. **6**(6): p. 443-450.

39. Rivera, W. and R.J. Romero, *Thermodynamic design data for absorption heat transformers. Part seven: Operating on an aqueous ternary hydroxide.* Applied Thermal Engineering, 1998. **18**(3-4): p. 147-156.

40. Rivera, W., M.J. Cardoso, and R.J. Romero, *Single-stage and advanced absorption heat transformers operating with lithium bromide mixtures used to increase solar pond's temperature.* Solar Energy Materials and Solar Cells, 2001. **70**(3): p. 321-333.

41. Zhao, Z., X. Zhang, and X. Ma, *Thermodynamic performance of a double-effect absorption heat-transformer using TFE/E181 as the working fluid.* Applied Energy, 2005. **82**(2): p. 107-116.

42. Kolda, T.G., R.M. Lewis, and V. Torczon, *Optimization by direct search: New perspectives on some classical and modern methods.* SIAM Review, 2003. **45**(3): p. 385-482.

43. Garousi Farshi, L., S.M. Seyed Mahmoudi, and M.A. Rosen, *Analysis of crystallization risk in double effect absorption refrigeration systems.* Applied Thermal Engineering, 2011. **31**(10): p. 1712-1717.

44. Zhang, D. and G.H. Lin, *Bilevel direct search method for leader-follower problems and application in health insurance.* Computers and Operations Research, 2014. **41**(1): p. 359-373.

45. Jradi, M., N. Ghaddar, and K. Ghali, *Experimental and theoretical study of an integrated thermoelectric-photovoltaic system for air dehumidification and fresh water production.* International Journal of Energy Research, 2012. **36**(9): p. 963-974.